The Cretaceous-Tertiary boundary in the Iberian Peninsula marine record: meteoritic impact phases, diagenesis and paleoenvironmental effects deduced from rock magnetism

El límite Cretácico-Terciario en el registro marino de la Península Ibérica: fases de impacto meteorítico, diagénesis y efectos paleoambientales deducidos del magnetismo de rocas

Víctor VILLASANTE MARCOS[1], Francisca MARTÍNEZ RUIZ[2],
María Luisa OSETE[3], Marcos A. LAMOLDA[4]

[1] Observatorio Geofísico Central
Instituto Geográfico Nacional
vvillasante@fomento.es

[2] Instituto Andaluz de Ciencias de la Tierra
CSIC-Universidad de Granada
fmruiz@ugr.es

[3] Dpto. Geofísica y Meteorología
Facultad de Ciencias Físicas, Universidad Complutense de Madrid
mlosete@fis.ucm.es

[4] Dpto. Estratigrafía y Paleontología
Facultad de Ciencias, Universidad de Granada
mlamolda@ugr.es

RESUMEN
Se ha investigado el magnetismo de rocas en cuatro secciones marinas del límite Cretácico-Terciario en la Península Ibérica. En Agost y Caravaca (SE España), con muy buen estado de preservación de la lámina de impacto que define el límite, la presencia en dicha lámina de espinelas ricas en Mg y Ni de origen meteorítico se evidencia por los aumentos en la susceptibilidad magnética y en la imanación remanente isoterma (IRM), acompañados de un descenso en la coercitividad de la remanencia. Esta fase ferrimagnética aparece junto a fases antiferromagnéticas de alta coercitividad, principalmente goethita de grano fino y hematites, originadas durante la diagénesis temprana en las condiciones anómalas posteriores al impacto. Los resultados indican un aumento del cociente terrígenos/carbonatos en el Daniense basal, seguido por la recuperación de la producción de carbonatos, llegando a exceder los

valores del Maastrichtiense terminal. Zumaya y Sopelana (N España) presentan estados de preservación peores de la lámina de impacto. En Zumaya existen restos de material de impacto adheridos a la capa de calcita que separa el Maastrichtiense de la arcilla del límite K-T. Dichos restos presentan aumentos de susceptibilidad e IRM y baja coercitividad de la remanencia, indicando la presencia de espinelas ricas en Mg y Ni. En Sopelana, donde no se hallaron restos de la lámina de impacto, no se detecta señal magnética de espinelas meteóricas; además, aunque el muestreo es demasiado limitado, los resultados apuntan también a una recuperación de la producción de carbonatos por encima de los valores del Maastrichtiense final.

Palabras clave: Límite K-T; impacto meteorítico; espinelas ricas en Ni; diagénesis temprana; goethita; paleoambiente; Agost; Caravaca; Zumaya; Sopelana.

ABSTRACT

Detailed rock magnetic properties of four sedimentary marine sections spanning the Cretaceous-Tertiary boundary have been investigated in the Iberian Peninsula. In Agost and Caravaca (SE Spain), which present a very good preservation state of the impact ejecta layer that defines the boundary, the magnetic fingerprint of impact-generated Mg-Ni-rich spinels is revealed by increases of one order of magnitude in magnetic susceptibility and isothermal remanent magnetization (IRM), associated with a decrease in coercivity of remanence. This dominant ferrimagnetic phase is accompanied by a significant amount of high-coercivity antiferromagnetic material, mainly goethite with very fine grain sizes and haematite, resulting from early diagenesis under the anomalous post-impact conditions. Rock magnetism supports a post-impact increase in the terrigenous/carbonate ratio during the early Danian, followed by a recovery of carbonate production that exceeds the end-Maastrichtian values. Zumaya and Sopelana (N Spain) present worst preservation states of the impact ejecta layer. In Zumaya some patches of impact material are found on top of the calcite layer that separates the end-Maastrichtian from the K-T boundary clay. In these patches, increases in susceptibility and IRM and a decrease in coercivity of remanence point to the presence of Mg, Ni-rich spinels of meteoritic origin. In Sopelana, no vestiges of the impact ejecta layer were found, and consequently there is no magnetic evidence of meteoritic Mg-Ni-rich spinels; although the sampled interval is too narrow, magnetic properties point to a recovery of carbonate production in the early Danian exceeding that of the end-Maastrichtian, in agreement with Agost and Caravaca results.

Key words: K-T boundary; meteoritic impact; Ni-rich spinels; magnesioferrites; early diagenesis; goethite; haematite; paleoenvironment; Agost; Caravaca; Zumaya; Sopelana.

1. INTRODUCTION

The events at the Cretaceous-Tertiary (K-T) boundary have received great attention because of the widespread biotic extinctions that mark the end of the Cretaceous, which represent the last of the five mass extinctions documented in the Phanerozoic record (Raup&Sepkoski, 1982; Jablonski, 1994; Sepkoski, 1996; MacLeod et al., 1997; Kiessling&Claeys, 2001; Sepkoski, 2002). Although several classic authors speculated as early as in the 18th century about the possible biotic effects of the impact of extraterrestrial objects against the Earth's surface (Maupertuis, 1750; Laplace, 1796), it was not until the paper of Laubenfels (1956) that a specific proposal of a meteoritic impact as the main cause of the K-T extinctions was made in a modern context. The first geochemical evidences of meteoritic impact at the K-T boundary, consisting of anomalously high abundances of iridium at a clay layer

separating Maastrichtian from Danian sediments in a variety of sedimentary sections around the world, were presented by Alvarez et al. (1980) and slightly later by Smit&Hertogen (1980). Since then, much information about this meteoritic impact, its magnitude and its traces in the sedimentary record has been recovered. Several geochemical, mineralogical and physical globally distributed markers are now recognized as solid proof of a meteoritic impact of great magnitude at the K-T boundary: geochemical anomalies, mainly high abundance of iridium and other Platinum Group Elements (PGE) (Alvarez et al. 1980; Smit&Hertogen 1980; Kyte et al. 1980; Ganapathy 1980; Kyte 2002; Claeys et al. 2002); presence of minerals with features corresponding to ultra-high pressure shock deformation (Bohor et al. 1984, 1987; Claeys et al. 2002); Os- and Cr-isotopic anomalies (Turekian 1982; Luck&Turekian 1983; Shukolyukov&Lugmair 1998; Quitté et al., 2003, 2007; Trinquier et al., 2006); tektites, microtektites and microkrystites with varying degrees of post-depositional alteration (Smit&Klaver 1981; Montanari et al. 1983; Smit&Kyte 1984; Sigurdsson et al. 1991; Smit et al. 1992; Kyte 2002); and presence of magnesium and nickel-rich spinels with varying compositions and high oxidation states, also reported in the literature as magnesioferrites (Smit&Kyte 1984; Kyte&Smit 1986; Robin et al. 1991, 1992; Kyte&Bostwick 1995; Robin&Rocchia, 1998). Indeed, the International Commission on Stratigraphy decided to place the base of the Danian (and hence the K-T boundary) at the very base of the thin reddish layer containing several of these impact markers in El Kef section, Tunissia (Molina et al., 2006).

In addition to these sedimentary markers, the sediment-covered, ≥180 km-wide impact structure of Chicxulub (Yucatan Peninsula, Mexico; Penfield&Camargo, 1981) has been recognized as the most probable source for the K-T boundary impact ejecta layer. The simultaneity of the K-T boundary with the Chicxulub impact event has been well established by radiometric dating of impact glasses recovered from various K-T boundary sections and of Chicxulub impact melt samples (Swisher III et al. 1992; Sharpton et al. 1992). Detailed geochemical studies indicate that both materials come from the same source (Hildebrand et al., 1991; Sigurdsson et al., 1991; Sharpton et al., 1992; Kring&Boynton, 1992) and consistent radiometric ages of zircons in the K-T boundary impact layer and in the Chicxulub impact breccias correspond to the pan-African, impact excavated continental basement of Yucatan (Krogh et al., 1993). The biostratigraphic dating of Chicxulub structure is consistent with the detailed biostratigraphy of the proximal ejecta deposits, indicating a K-T boundary age (Arz et al., 2004; Arenillas et al., 2006). Finally, the magnetostratigraphic data obtained from Chicxulub drilled materials are consistent with a K-T boundary age (Sharpton et al., 1992; Urrutia-Fucugauchi et al., 1994; Rebolledo-Vieyra&Urrutia-Fucugauchi, 2006), which is placed in the upper half of magnetochron C29R (Cande&Kent, 1995). Although it is thus well established that an extraterrestrial object of ~ 10 km in diameter impacted Earth's surface at the K-T boundary with global consequences, its environmental and biotic effects and its role in the end-Cretaceous mass extinction are controversial.

A few works have focussed on the rock-magnetic properties of K-T boundary material, with different scopes and different degrees of detail. Worm and Banerjee (1987) measured several magnetic parameters in bulk sample and in magnetic microspherules from the impact layer of Petriccio section (Italy), and surface magnetic susceptibility in Pacific and Indian Oceans DSDP sedimentary cores. Similarly, Cisowski (1988; 1990) determined rock magnetic properties of five magnetic microspherules from Petriccio and of bulk samples from a variety of continental and marine sections. Although there are some differences between these works, they agree pointing to the impact-generated magnesioferrites or Mg, Ni-rich spinels as the main magnetic phase within the K-T boundary microspherules. Morden (1993) conducted rock magnetic experiments in the K-T boundary Fish Clay of Stevns Klint (Denmark), both in bulk sample and in a magnetic extraction. The Curie curves of the magnetic extraction showed the presence of some Fe particles, with low Ni-content, interpreted by the author as low-Ni iron spherules originated from the vaporized K-T impactor. In other studies bulk magnetic susceptibility has been used as a proxy for $CaCO_3$ content and climatic cyclicity in marine sediments of Zumaya section in northern Spain (Ten Kate&Sprenger, 1993) and four DSDP K-T boundary sections in the southern Atlantic Ocean (D'Hondt et al., 1996), detecting increases in the magnetic susceptibility of the K-T boundary clay layer.

Other techniques apart from rock magnetism have been used to specifically address the characterization of iron-rich phases in the K-T boundary. Griscom et al. (1999) applied electron spin resonance to K-T boundary material and reported anomalous increases of ferromagnetic resonance intensity in Caravaca (Spain), Sopelana (Spain) and Gubbio (Italy). The results were interpreted as indicating the presence of spherical fine-grained (~ 4-5 nm) magnetite particles, suggested to come from weathered glass spherules produced by the Chicxulub impact. After distribution and deposition, this glass would transform to clay, but the proposed magnetite particles pervading it would survive. Brooks et al. (1985) used X-ray diffraction and Mössbauer spectroscopy to analyze bulk samples and iron-oxide spheroids from the K-T boundary at Woodside Creek (New Zealand). They identified microcrystalline goethite (10-20 nm) in the matrix and crystalline goethite (> 200 nm) and some haematite in the spheroids. Based on geochemical data, the authors interpreted these magnetic phases as authigenic products, probably formed from pyrite clumps originated in the very reducing post-impact environment. Wdowiak et al. (2001) have recently used Mössbauer spectroscopy in several K-T boundary sections, identifying widespread superparamagnetic phases reported to be goethite with various particle-sizes up to few tens of nanometres, except in some sections where they are reported as haematite. The authors speculated with the possibility that this nanophase could be the iridium K-T boundary carrier and that it originated from condensation of a chondritic vaporized impactor inside a vapour impact plume. Mössbauer spectroscopy has been applied also by Verma et al. (2001) and Bhandari et al. (2002), who again identified superparamagnetic phases reported as iron oxides/oxyhydroxides like haematite and goethite. These authors support a meteoritic origin of this Fe-nanophase in the form of iron nanoparticles

condensed from the impact vapour cloud, deposited globally and subsequently weathered to oxides/oxyhydroxides. Neither these authors, nor Wdowiak et al. (2001), provided any conclusive data in support of their assertions about a meteoritic, primary origin of the superparamagnetic phases. Specifically, they do not seem to consider a potential diagenetic origin, as was otherwise concluded by Brooks et al. (1985) based on additional geochemical information.

Later, Villasante-Marcos et al. (2007) have investigated rock-magnetic properties of K-T boundary material from a variety of sections with different distances to Chicxulub impact structure, from proximal (El Mimbral and La Lajilla, Mexico), through intermediate (Blake Nose, ODP Leg 171, western North Atlantic) to distal (Agost and Caravaca, Spain). They detected both a strong ferrimagnetic phase, identified as the Mg, Ni-rich spinels of meteoritic origin, and also high coercivity antiferromagnetic phases dominated by fine grained goethite with a significant superparamagnetic fraction. Based on detailed geochemical and iridium data on proximal and intermediate sections, the authors unambiguously rejected this high coercivity phase as the iridium carrier and provided strong support for a diagenetic origin, in agreement with the model suggested by Brooks et al. (1985) for Woodside Creek. This paper presents improved results about the rock magnetic properties of Agost and Caravaca, as well as new unpublished data from Zumaya and Sopelana.

2. STUDIED SECTIONS

Agost and Caravaca sections belong to the External Zones of the Betic Cordillera (SE Spain), and can be considered as twin sections, although Caravaca was originated in a deeper sedimentary environment and certain differences occur in the diagenetic history experimented by the very thin red clay layer that defines the K-T boundary (Martínez-Ruiz et al., 1999). Both sections developed in a pelagic, continental slope environment (Figure 1), and the sediment deposition during the late Maastrichtian and the early Danian resulted in sequences of marls and marly limestones. The K-T boundary is marked in both sections by a reddish clay layer ~ 2 mm thick which represents the meteoritic-rich dust dispersed and deposited globally after the impact event, called hereinafter the impact layer. Above this thin layer a greenish to greyish clay layer ~ 5 to 15 cm thick was deposited as a result of the sudden decrease in ocean productivity. Its carbonate content gradually increases giving way to the Danian marly lithologies. In Agost, a marl rich layer ~2 cm thick is found intercalated within the upper part of the K-T boundary clay; this layer is not sharply defined and has not complete lateral continuity. Within the reddish impact layer several impact markers have been found: iridium spike and other geochemical anomalies (Smit&Hertogen, 1980; Smit&ten Kate, 1982; Martínez-Ruiz et al., 1992; Martínez-Ruiz, 1994); shocked quartz grains (Bohor et al., 1987); Mg- and Ni-rich spinels (Bohor et al., 1986; Robin et al., 1991); and microspherules considered to be diagenetically altered microkrystites (Smit&Klaver, 1981; Martínez-Ruiz, 1994; Martínez-Ruiz et al., 1997). These microspherules, with mean

sizes between 100 and 500 microns, are composed either of iron-oxide (Fe-O spherules) or K-feldspar, and their relative abundance establishes a difference between the two sections. Iron-oxide spherules are recovered from Agost section and are absent in Caravaca, where some scarce iron-oxide particulates or concretions occur but with no spherical shapes and in low quantities, mostly corresponding to altered pyrite framboids. K-feldspar spherules are recovered from both sections (Smit&Klaver, 1981; Martínez-Ruiz, 1994; Martínez-Ruiz et al., 1997). In some K-feldspar spherules, inner carbon-rich cores are detected and interpreted as a relict of the original material composing the microkrystites (Martínez-Ruiz, 1994; Martínez-Ruiz et al., 1997), suggesting a carbonaceous chondrite as the K-T boundary impacting body.
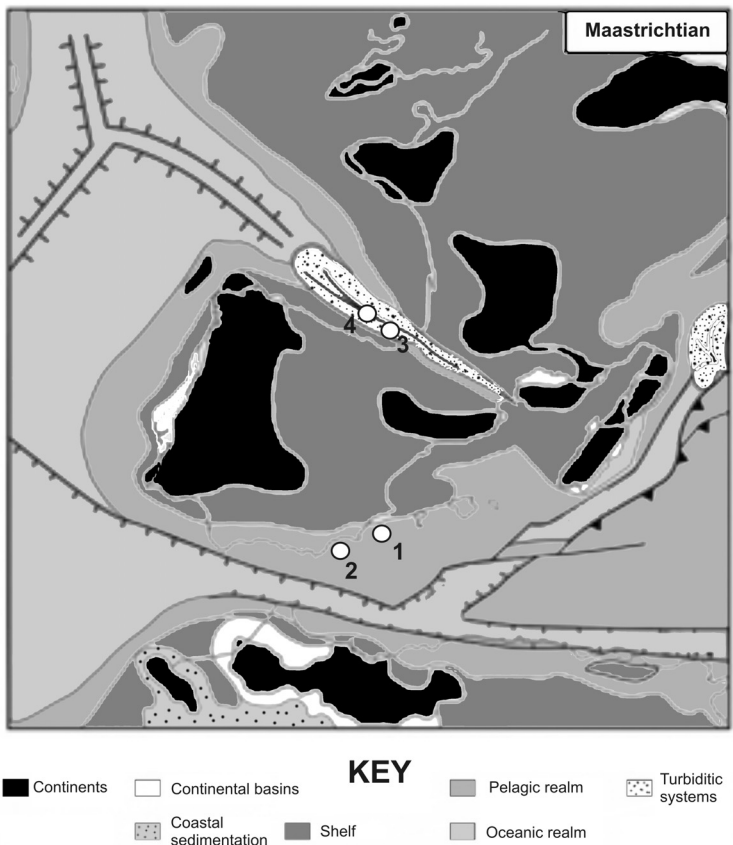

Figure 1. Paleogeographic location of the studied sections: 1) Agost (Alicante), 2) Caravaca (Murcia), 3) Zumaya (Guipuzcoa), 4) Sopelana (Vizcaya). Paleogeography from Martín-Algarra&Vera (2004).

Zumaya and Sopelana are located in the Basque-Cantabrian shoreline and belong to the Western Pyrenees units, consisting of uplifted and folded sedimentary rocks once deposited in the Basque-Cantabrian Region, in a westward-deepening marine basin which separated the European and Iberian plates and accumulated sediments until its closing at the end of the Eocene, produced by the Euro-African convergence. Both sections represent hemipelagic settings during the end-Maastrichtian and early Danian. In Zumaya (Baceta&Pujalte, 2006), the upper Maastrichtian is characterized by alternations of purple marls and grey marly limestones with intercalated siliciclastic turbidites; the Danian is represented by alternation of pink-grey limestones and marls with some thin calcareous turbidites. The K-T boundary is marked by a 7-8 cm thick grey marly clay layer. Due to tectonic interbed sliding, calcite slickensides 1-2 cm thick have deposited both at the bottom and at the top of the clay-rich interval, irregularly altering the basal part of the K-T boundary marly clay. This resulted in a serious alteration of the impact layer, which can be observed only as irregular patches of yellowish to brownish silty material adhered to the top of the basal calcite layers. Within these rests of impact layer, iridium and Ni-rich spinels are detected (Martínez-Ruiz, 1994; Rocchia et al., 1996). In Sopelana (Lamolda et al., 1983; Mary et al., 1991), the uppermost Maastrichtian is represented by grey marls and marly limestones; they are followed by a ~ 30 cm thick darker, clay-rich marl layer, corresponding to the K-T boundary clay, which gives way to a hard limestone layer and to the Danian marl-limestone succession. Although the basal ~2 cm of the clay-rich K-T boundary marls present a reddish colour, no evident impact layer seems to have been preserved at Sopelana, at least in the part of the section studied and sampled in this work. Nevertheless, high iridium abundances are present in the basal part of the clay-rich layer (Rocchia et al., 1988; Martínez-Ruiz, 1994), as well as other geochemical and carbon and oxygen isotopic anomalies (Martínez-Ruiz, 1994).

3. METHODOLOGY

Samples were taken from cleaned outcrop exposures (Agost, Caravaca and Sopelana) or from naturally exposed fresh rock surfaces (Zumaya), in order to minimize weathering disturbing effects. To separate material from the thin impact layer, block samples spanning the last Maastrichtian and the first Danian centimetres and sandwiching the impact layer were taken and brought to the laboratory. There, impact layer material was mechanically separated with non-magnetic tools, as well as material directly below and above the impact layer. The rock magnetic experiments have been conducted in the Paleomagnetism Laboratory of the Complutense University of Madrid (Spain). Bulk magnetic susceptibility was measured with a KLY-3 Kappabridge (Agico). Each sample was measured ten times and averaged; the measurement error is estimated by the standard deviation (σ), which is always small (relative error is less than 10% for weak samples and between 0.1 and 1 % for strongly magnetic samples).

Sub-samples from all samples were subjected to systematic treatment with a Coercivity Spectrometer (Jasonov et al., 1998), obtaining induced-magnetization (hysteresis) and remanent-magnetization (IRM) cycles up to 0.5 T; field steps of 0.5 mT were used and each data point was measured 9 times and averaged. For this treatment, fragments of material were packed in gelatine capsules, wrapped in paper and fixed to the instrument holder. An empty capsule with wrapping paper was previously measured and its signal subtracted from samples' curves. For weak magnetic samples these curves present a very significant instrumental noise, making it necessary to use improved ways to calculate the usual magnetic parameters and to estimate associated errors, in order to be able to compare different samples. From the IRM curves, several parameters were calculated, and their errors estimated, as following:

- The Isothermal Remanent Magnetization acquired under the maximum applied magnetic field of 0.5 T (IRM_{500mT}) was calculated as the mean value of the remanent magnetization acquired between fields of 500 and 400 mT in the $H_{max}>H>0$ branch of the cycle. This procedure minimizes the effect of instrumental noise for magnetically weak samples. The error associated to IRM_{500mT} is the standard deviation (σ) of the mean.
- The coercivity of remenence (H_{cr}) was calculated fitting a linear trend to the back-demagnetization part of the remanent curve in the region where it crosses the *H*-axis ($M_r = 0$). We calculate the point where this linear trend intersects the *H*-axis, and this value corresponds to H_{cr}. If the equation of the linear trend is $M_r = m \cdot H + n$ (where M_r is the remanent magnetization and H is the applied magnetic field), the estimated coercivity of remanence is $H_{cr} = -n/m$. Its associated error has been estimated by a first order approximation of the error propagation, which gives $\Delta H_{cr} = \left| \Delta n/m \right| + \left| n\Delta m/m^2 \right|$, where Δn and Δm are the errors of the linear fit. To this ΔH_{cr} value, we add an additional constant error of 1 mT which comes from the variability of the holder + gelatine capsule + wrapping paper signal subtracted from all the samples. To estimate this variability, we measured the holder with 10 different empty capsules and 10 different pieces of wrapping paper.
- The S_{100mT} ratio is the quotient between the IRM acquired under a back-demagnetization field of 100 mT and the IRM_{500mT}. The IRM_{-100mT} is estimated fitting a linear trend to the curve in the region between applied fields of -90 and -110 mT and calculating the linear M_r value at the middle point $H = -100$ mT. The associated error of IRM_{-100mT} is calculated as in the case of the coercivity of remanence. After that, we calculate $S_{100mT} = -IRM_{-100mT}/IRM_{500mT}$ and its associated error is again estimated by

$$\Delta S_{100mT} = \left| \Delta IRM_{-100mT}/IRM_{500mT} \right| + \left| IRM_{-100mT} \cdot \Delta IRM_{500mT}/IRM_{500mT}^2 \right|$$

With this procedure we improve the calculation of magnetic parameters for weak samples and we estimate their associated errors with generosity (we expect the real errors to be generally smaller than our estimations), allowing us to compare different weak samples with enough certainty.

Additional IRM acquisition curves were obtained for selected Agost and Caravaca samples using an ASC Scientific Model IM-10-30 impulse magnetizer to impart the magnetization and a JR5-spinner magnetometer (Agico) to measure it. In this case, maximum applied magnetic fields exceeded 2 T, reaching 4.92 T for Agost K-T boundary impact layer sample. Quantitative analysis of coercivity distributions for some selected samples was performed with the CODICA 5.0 software developed by R. Egli (Egli, 2004 a, b; Egli, 2005). Magnetic component analysis was performed with GECA 2.1 software, by the same author, from the coercivity distributions obtained with CODICA. The unmixing procedure of GECA makes use of skewed generalized Gaussian distributions (SGG), determined by the usual two parameters MAF (median acquisition field) and DP (dispersion or standard deviation), similar to those that define the centre and the wideness of a log-normal Gaussian distribution, plus the two additional parameters skewness (s) and kurtosis (k), which define the degree of asymmetry and the curvature of the corresponding SGG function. This analysis is naturally developed in a *logH* scale, where the applied magnetic field *H* is transformed to $h = logH$, and the remanent magnetization $M_r(H)$ is correspondingly transformed to $M_r*(h) = ln10 \cdot 10^h \cdot M_r(10^h)$. Results are presented for some selected samples measured with the Coercivity Spectrometer. The analysis has been performed on the back-demagnetization branch of the curves after its inversion and normalization, and the focus is placed on the MAF and DP values.

Thermal demagnetization of an IRM imparted along three orthogonal axes (Lowrie, 1990) was performed for a selected set of samples with the use of an ASC Scientific Model IM-10-30 impulse magnetizer, a Schonstedt TSD-1 furnace and a JR5 spinner magnetometer. Bulk magnetic susceptibility was measured after each temperature step to monitor mineralogical changes during heating. To carry out this experiment, the original irregular non-compacted sediment samples were slightly pulverized in an agate mortar, mixed with sodium silicate (water glass) and dried in air at ambient temperature, to obtain solid, easily oriented cylindrical samples. This procedure served for most of the samples, but especial problems had to be solved to prepare an extraction of iron-oxide microspherules from Agost impact layer. To extract the spherules we obtained the solid residue from the bulk sample by disaggregating it, diluting it in water, waiting for the heavy fraction to deposit and washing away the suspended clay fraction. After that we used a binocular lens, precision entomological pincers and a single-hair paintbrush moistened with alcohol to separate one by one a significant number of iron-oxide microspherules (maximum size ~ 500 microns). Although we obtained enough quantity to measure hysteresis cycles and thermomagnetic curves, we had to mix the remaining microspherules with a matrix material to make a compacted cylindrical sample and to subject it to the IRM thermal demagnetization experiment. As matrix material we used finely pulverized cretaceous marl from the Agost sample situated between -15 and -20 cm, which

showed low susceptibility and low IRM_{500mT}. As a control test, we prepared a similar sample completely made of the marly matrix and we subjected it to the same IRM thermal demagnetization experiment, allowing us to subtract the matrix signal from the microspherules + matrix curves (in proportion to the mass fraction of the matrix).

Thermomagnetic curves for selected samples were obtained with a Variable Field Translation Balance (MMVFTB, Magnetic Measurements Ltd.). Heating was conducted in air and maximum temperatures of 800º C were reached. Cooling curves were measured to monitor mineralogical irreversible changes.

Magnetic extraction was performed both in Agost and Caravaca impact layer samples. Two different methods were used. The most sophisticated ("peristaltic pump") consisted in the circulation of sediment diluted in distilled water inside a close circuit, passing beside a magnetic trap. The magnetic trap was made with commercial neodymium-boron strong magnets placed inside a glass tube immersed in the water, and the water circulation was slowly driven by a peristaltic pump. This method proved to be highly inefficient, requiring running times of around 6-7 days to obtain an exiguous magnetic residue. A much better and simpler method ("hand magnet") consisted in diluting the sediment in a small recipient full of distilled water and moving the magnets, placed in a plastic bag, through the water-sediment mixture. The magnetic particles adhered to the plastic were subsequently washed with distilled water to a clean recipient, and they were recovered after drying at ambient temperature. In addition, scarce and irregular iron-oxide concretions were mechanically separated from Caravaca impact layer, by the same procedure used to separate Agost Fe-O spherules. Susceptibility, hysteresis cycles, IRM curves and thermomagnetic curves were measured for the magnetic extractions and Caravaca Fe-O concretions.

Most of the results are presented as stratigraphic plots of four magnetic parameters: χ, IRM_{500mT}, H_{cr} and S_{100mT}. Error bars in the *y*-axis represent the different stratigraphic intervals included and homogenized in each sample. Error bars in the *x*-axis have been included for all the parameters, but for χ and IRM_{500mT} they are generally smaller than the size of data-points and can not be appreciated.

4. RESULTS

In Figure 2, a stratigraphic plot of mass-specific bulk magnetic susceptibility (χ), IRM_{500mT}, H_{cr} and S_{100mT} is shown for Agost section. The impact layer presents values of χ and IRM_{500mT} about one order of magnitude higher than surrounding material, indicating a very significant increase in ferromagnetic content. This magnetic spike is connected to a low H_{cr} (~16 mT) and S_{100mT} close to 1, indicating that a low coercivity ferrimagnetic phase is dominating the magnetic fingerprint of the impact layer. The samples immediately below and above the impact layer also show low H_{cr} values, although χ and IRM_{500mT} are not high. For the two samples directly contiguous to the impact layer, this could indicate contamination with impact layer material during the sample separation process. But for the others it seems instead to

indicate that the original stratigraphic distribution of the low coercivity ferrimagnetic phase was not strictly confined to the impact layer, but spanned also the last centimetres of the Maastrichtian and the first centimetres of the Danian, with lower concentrations. White circles in Figure 2 represent values for the Fe-O microspherules extraction. As can be seen, χ and IRM_{500mT} values for the microspherules are high, but lower than bulk impact layer sample values, H_{cr} is high and similar to Maastrichtian and Danian values, and S_{100mT} is significantly lower (~ 0.3). This indicates that the microspherules have a ferromagnetic content higher than Maastrichtian or Danian material, but lower than impact layer bulk sample, and that they have a high fraction of high coercivity antiferromagnetic material, in contrast with the impact layer bulk sample which is dominated by a ferrimagnetic phase. Therefore, the magnetic behaviour of bulk impact layer sample can not be explained by dissolution of Fe-O magnetic microspherules within a less magnetic matrix, but a high abundance of fine ferrimagnetic material dispersed within the matrix has to be present.

   In Figure 3, normalized IRM acquisition curves for Agost samples are shown, both for the Coercivity Spectrometer (all samples, up to 0.5 T) and the impulse magnetizer (selected samples, up to > 2 T) experiments. As can be seen, all samples show major contributions from low-coercivity ferrimagnetic phases, but the coercivity spectra of the impact layer sample is clearly displaced to lower fields. In addition, all samples show a significant contribution from high-coercivity phases. The relative importance of the high-coercivity phase is generally higher in Maastrichtian and Danian samples, and lower in the impact layer sample, as previously deduced from S_{100mT} behaviour. The complete IRM acquisition and back-demagnetization curve for the Fe-O microspherules extraction in Figure 3D shows a very significant contribution from a high-coercivity phase with a rather apparent relaxation of the IRM in the $H_{max}>H>0$ branch over timescales of less than ~ 6 minutes. This, together with X-ray diffraction patterns published by Villasante-Marcos et al. (2007), indicates a dominance of fine grained goethite with a high superparamagnetic fraction within the Fe-O microspherules. Nevertheless, an important low coercivity ferromagnetic fraction is also present in the microspherules.
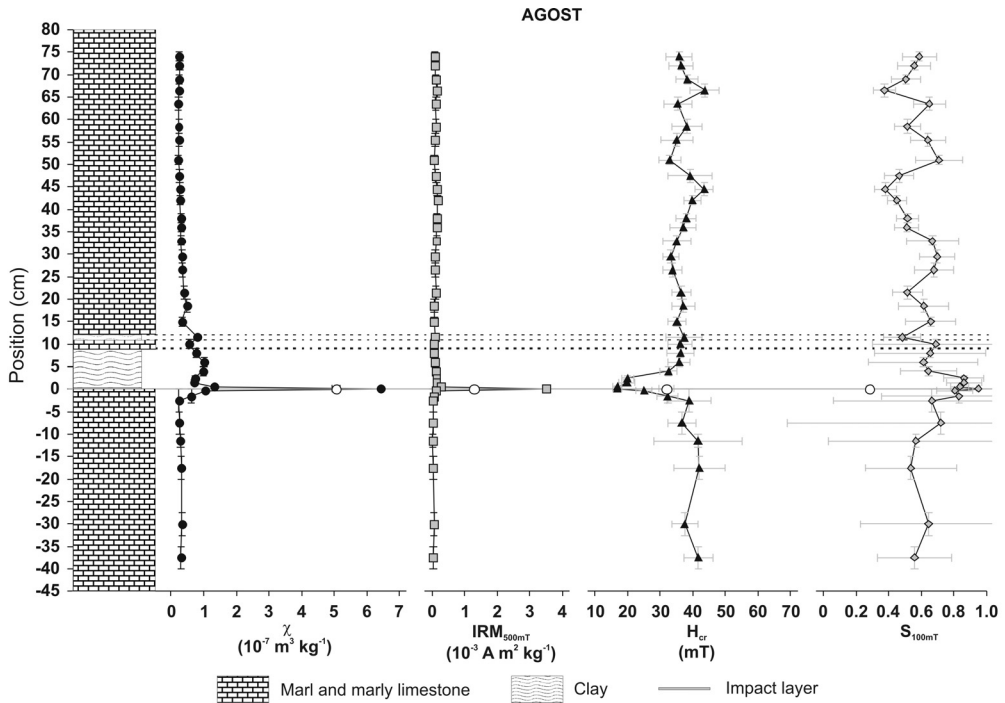
Figure 2. Agost rock magnetic parameters for bulk samples and Fe-O microspherules extraction (white circles).

Figure 4 presents 3-axis IRM thermal demagnetization and Curie curves for Agost impact layer, Fe-O microspherules and hand-magnet magnetic extraction. The IRM of the impact layer bulk sample is mainly concentrated in the 0.12 T axis and shows a continuous decrease up to 450-500º C, with probable partial falls around 150, 300 and 450º C. This indicates a more or less continuous range of unblocking temperatures for the low-coercivity dominant component below 500º C. The 2 T axis shows a small but resolvable contribution of high coercivity phases, with a little inflexion below 100º C indicating the presence of goethite, and a main fall at 675º C due to the presence of haematite. The 0.4 T axis shows no significant contribution. The thermomagnetic curve for the impact layer shows a steep decrease below 100º C, a partial fall between 300 and 350º C, a continuous decrease up to 600º C, and a different cooling curve with an inflexion at 650º C. The two first features, and the characteristics of the cooling curve, point to the presence of goethite with a Curie point below 120º C, which subsequently dehydrated above 300º C to form haematite. Both experiments indicate that Agost impact layer is dominated by a low coercivity component with a range of unblocking and Curie/transformation

temperatures up to 450-500º C. Additionally, goethite and haematite are also present in significant amounts.

Agost Fe-O spherules data show an IRM concentrated in the 2 T axis with falls below 150º C, at 250-300º C and at 650º C, indicating that goethite and haematite dominate their magnetic properties. In the 0.3 and 0.1 axis, IRM shows inflexions at 100º C and partial falls at 300º C and 650º C, indicating the presence of goethite and haematite fractions with low coercivities. The thermomagnetic curve shows clearly the goethite signature: steep decrease below 100º C, transformation around 300º C and the 650-675º C Curie point of haematite, which could be either original or newly formed from the goethite
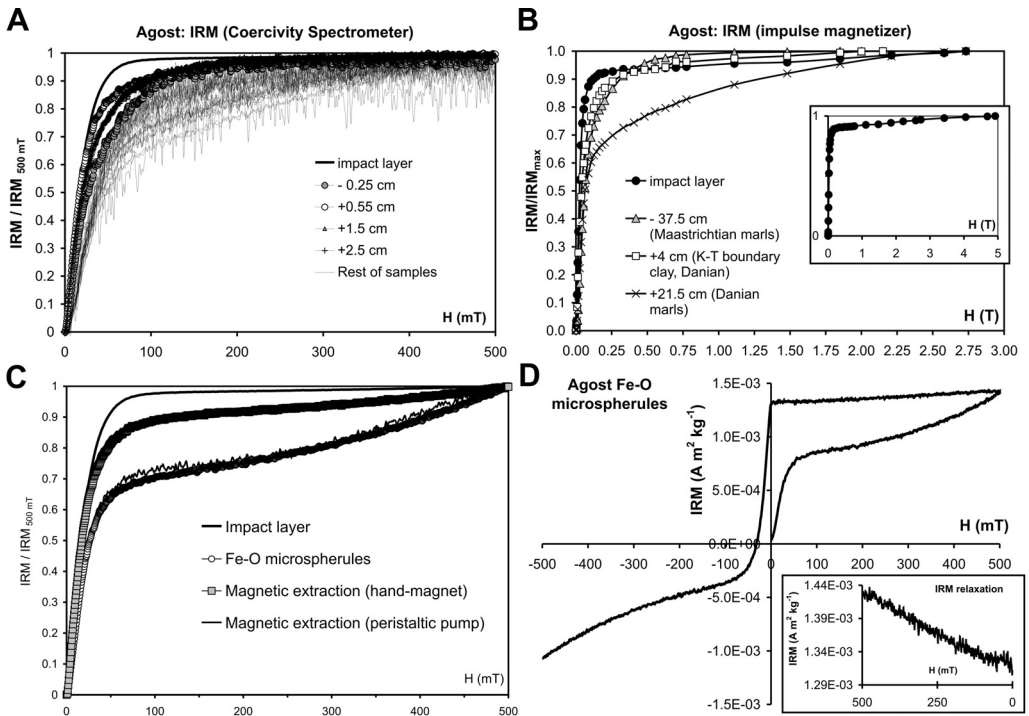
Figure 3. A) IRM back-demagnetization curves (rescaled and normalized) for Agost samples, Coercivity Spectrometer up to 0.5 T. B) IRM acquisition curves, impulse magnetizer up to > 2 T; inset, IRM curve for Agost impact layer up to 4.9 T. C) IRM back-demagnetization curves for Agost impact layer, Fe-O microspherules and magnetic extractions (Coercivity Spectrometer, up to 0.5 T). D) IRM acquisition and back-demagnetization curve for iron-oxides microspherules extraction; inset, IRM relaxation in the 0<H<H$_{max}$ branch (Coercivity Spectrometer, up to 0.5 T).

Two thermomagnetic curves are shown for Agost hand-magnet magnetic extraction (Figure 4E, F). The first was obtained under an external applied field of 1 T, which should affect both low and high coercivity phases. Irreversible behaviour is detected as before, with different heating and cooling curves. Decreases below 100º C and at 300-350º C in the heating curve indicate presence of goethite, but a new feature is the appearance of an increase between 500 and 550º C, signalling the generation of a new magnetic phase with a quasi-linear range of Curie temperatures below 550º C (as evidenced by the cooling curve) and with higher intensities. The second curve (Figure 4F) was obtained with an external field of 75 mT, which should affect strongly any low coercivity phase but leave less affected the high coercivity phases. The signature of goethite is thus almost suppressed (just a slight decrease around 350º C, indicating thermally driven dehydration), and the peak due to the generation of the new magnetic phase is strongly enhanced. This peak occurs between 450 and 525º C, and the magnetization subsequently and dramatically falls between 525 and 575º C. The cooling curve indicates that the new phase has a much higher magnetization (note that the magnetization scale is logarithmic). All this shows that a new strongly magnetic, low-coercivity phase is created under heating over 450º C, its Curie point below 600º C pointing to magnetite. All these features (and the absence of Verwey transition reported by Villasante-Marcos et al., 2007) can be explained by the presence of highly oxidized (maghemitized) magnesioferrites (Mg, Ni-rich spinels) accompanied by a high proportion of goethite and haematite, which seem to be concentrated within the Fe-O spherules. The Mg, Ni-rich spinels have to be mainly present as fine material dispersed within the bulk sample, although some fraction could reside in the Fe-O microspherules; they should have reduced magnetizations and Curie points, compared with those of pure magnetite. The generation of newly formed magnetite under heating the magnetic extraction over 450º C could be due either to irreversible alteration of the oxidized spinels (deoxidization) or to alteration of Fe-containing paramagnetic material originally adhered to the impact layer ferromagnetic phases and thus dragged by the later into the magnetic extraction.
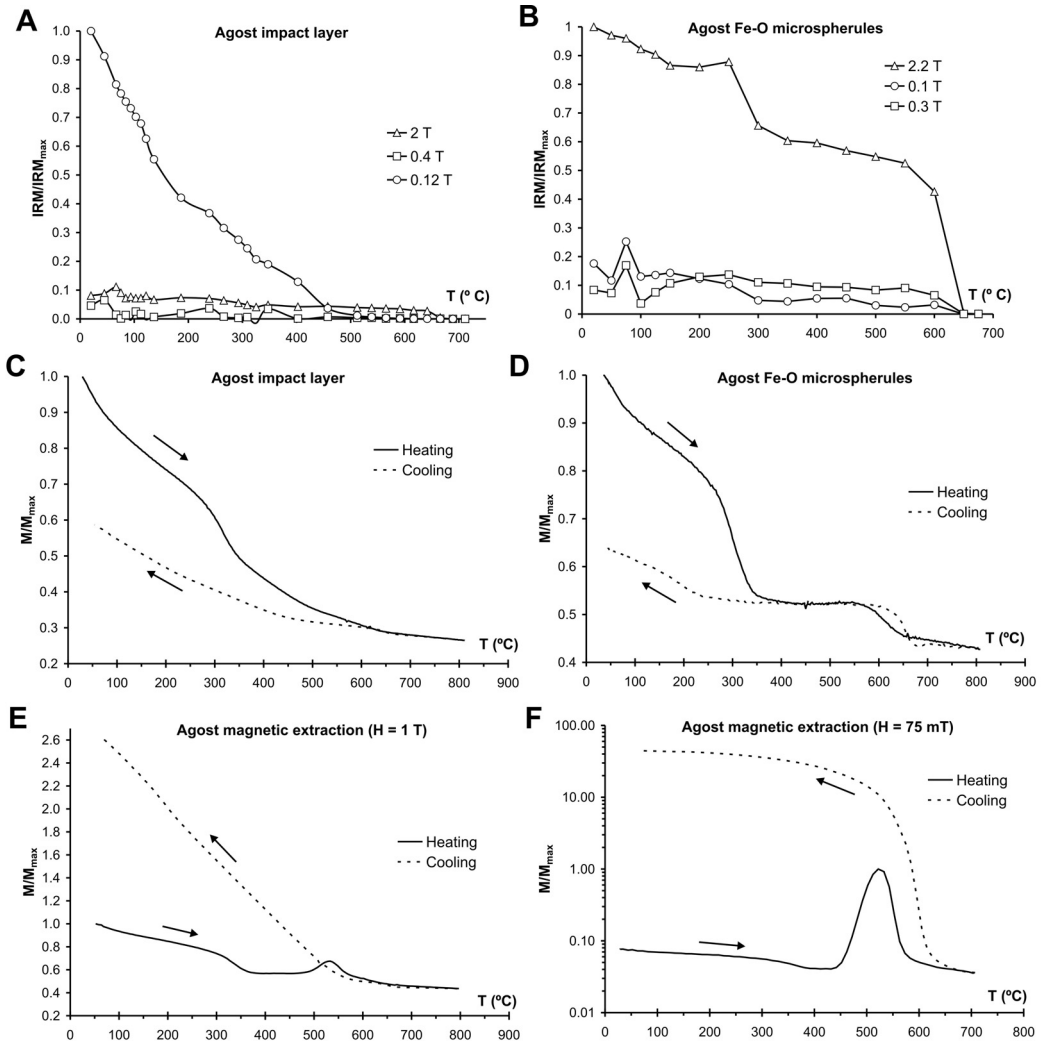
Figure 4. A) 3-axis IRM thermal demagnetization for Agost impact layer. B) 3-axis IRM thermal demagnetization for Agost Fe-O microspherules extraction. C) Thermomagnetic curve for Agost impact layer (field 1 T). D) Thermomagnetic curve for Agost Fe-O microspherules extraction (field 1 T). E) Thermomagnetic curve for Agost hand-magnet magnetic extraction (field 1 T). F) Thermomagnetic curve for Agost hand-magnet magnetic extraction (field 75 mT; magnetization scale is logarithmic, to allow proper visualization of heating and cooling curves).

In order to analyze any paleoenvironmental trend revealed by the stratigraphic variation of rock magnetic parameters, we have re-drawn Figure 2 without the values of the impact layer, the two immediately overlying samples and the immediately underlying sample, thus eliminating the magnetic signature of the impact material. The result is shown in Figure 5. A very clear trend in susceptibility is observed: Maastrichtian material shows low susceptibility values and the K-T boundary clay is marked by an increase in susceptibility, subsequently decreasing in the first Danian marls. Low Danian background values seem to be reached again after ~ 45 cm, but they are slightly lower than Maastrichtian background values. The IRM_{500mT} behaves differently, with possibly an increasing trend within the Danian and significant fluctuations. Although H_{cr} does not show any definite trend (considering the error bars), it also presents fluctuations coupled with IRM, high values of IRM showing higher coercivities. S_{100mT} is clearly negatively coupled with H_{cr}, as expected. To investigate the possible correlation of these features with the carbonate content of the sediments, we used carbonate fraction data from Martínez-Ruiz (1994). Figure 6 shows χ and IRM_{500mT} in a carbonate-free basis, together with non-carbonate fraction. After the carbonate correction the susceptibility increase in the K-T boundary clay and its subsequent decrease during the first Danian marls disappear, indicating that this feature was due to carbonate content variation. Instead, a general increasing trend similar to the IRM is retained, pointing to a fluctuating increase of ferromagnetic fraction in the lower Danian. On the other hand, the magnetic spike associated with the impact layer is maintained after carbonate correction. This, as shown also by the H_{cr} decrease, demonstrates that the impact layer magnetic spike is not due to the dramatic fall of carbonate content, but to the presence of a distinct low-coercivity phase in the impact layer and possibly in the first centimetres of the K-T boundary clay and the last centimetres of the Maastrichtian.
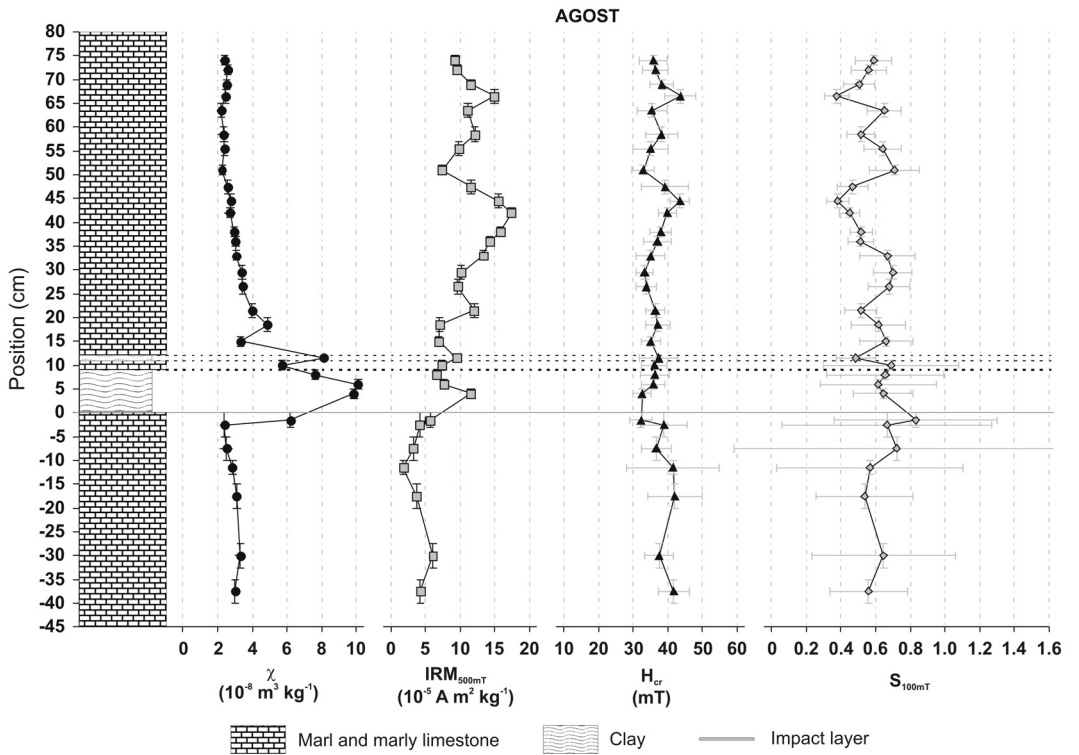
Figure 5. Agost magnetic parameters after eliminating data-points from impact layer and contiguous samples.
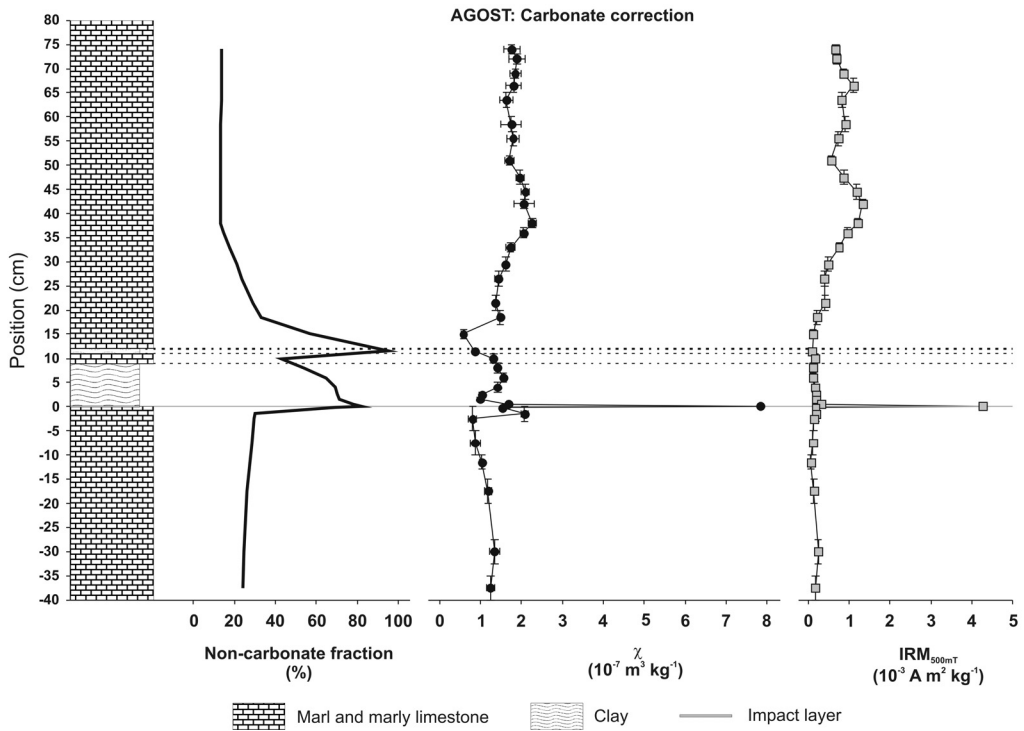
Figure 6. Agost χ and IRM_{500mT} in a carbonate free basis, together with non-carbonate fraction.

Results for Caravaca are very similar to Agost. The impact layer is associated with a peak in χ and IRM_{500mT}, a low H_{cr} and an S_{100mT} ratio close to 1 (Figure 7). The sample immediately overlying the impact layer presents also high susceptibility and IRM, although not as high as the impact layer, and low coercivity of rema-nence, indicating that the low coercivity phase responsible of the impact layer mag-netic spike is also present in the first cm of the K-T boundary clay, either as con-tamination during sample preparation or as an original phase not confined to the impact layer. Figure 8 shows normalized IRM curves, 3-axis IRM thermal demag-netization and thermomagnetic curves for Caravaca. Impact layer sample is domi-nated by a low-coercivity phase with a coercivity distribution displaced towards low fields, when compared with the low-coercivity phases present in Maastrichtian and Danian samples. No significant contribution from high coercivity phases is seen in the IRM curve of the impact layer, although all the other samples show varying fractions of high coercivity phases. The coercivity distribution of the first Danian sample is similar to that of the impact layer, pointing again to the existence in the first Danian cm of the characteristic low coercivity phase. Magnetic extraction

(hand magnet) behaves similarly to bulk impact layer sample, with the coercivity distribution slightly displaced to still lower fields.

Iron oxide concretions found in Caravaca impact layer (see description of sections) were separated by the same procedure used with Agost microspherules and its IRM was measured (Figure 8A); they are clearly different from Caravaca bulk impact layer sample and also from Agost Fe-O spherules. Instead, they behave similarly to Caravaca Maastrichtian and Danian samples; they do not show evidence of the low coercivity component characteristic of the impact layer, but an evident strong contribution of high coercivity material is observed. Some relaxation of the IRM is observed in the $H_{max} > H > 0$ branch, amounting to a total of around 4% of the IRM_{500mT}, but it begins after the applied magnetic field decreases below 300 mT and it is really strong only after H decreases below 100 mT (compare with the Agost Fe-O spherules IRM relaxation, which amount to 10% and begins at fields below 500 mT). This points to the presence of some superparamagnetic material in the concretions, but with either lower coercivities or with greater relaxation times than Agost Fe-O spherules.
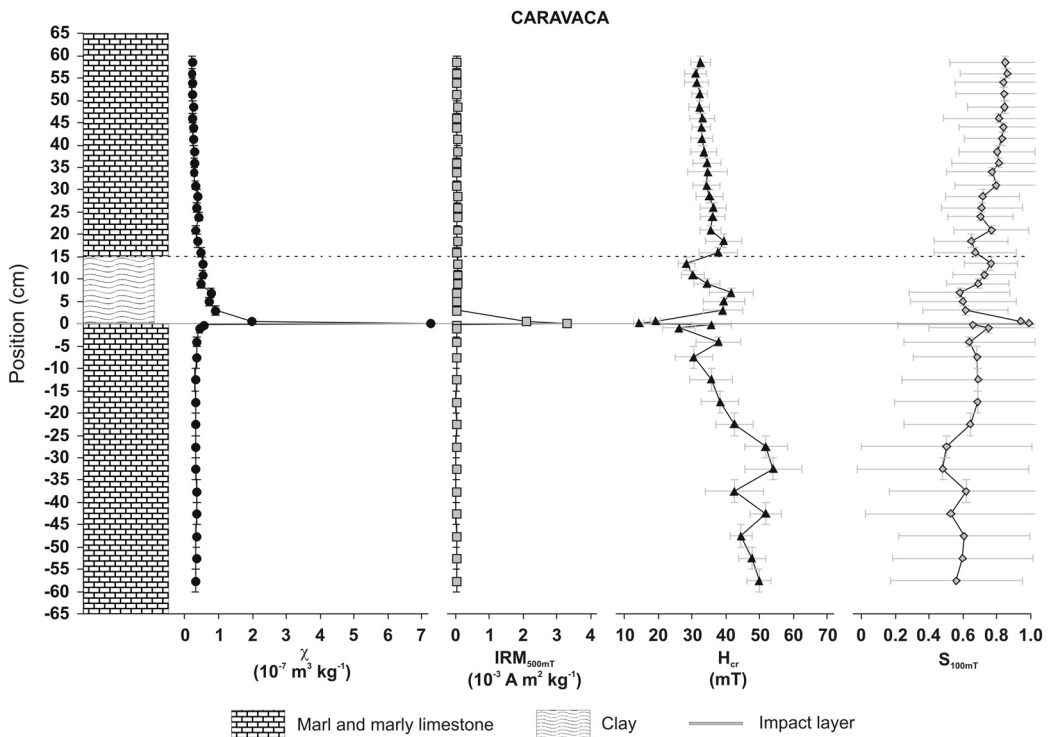

Figure 7. Caravaca rock magnetic parameters for bulk samples.

Figure 8D shows that the IRM of impact layer is concentrated in the 0.12 T axis and it falls to zero at 570º C, with partial falls below 100º C and at 150, 300 and 450º C. No resolvable fraction of the IRM is retained in the 0.4 and 2 T axis. The thermomagnetic curve (Figure 8E) is again irreversible, indicating mineralogical changes during heating. Magnetization falls gradually below 500º C, and an increase above 500º C denotes the generation of a new magnetic phase which is more magnetic and shows a linear range of Curie temperatures below 500-550º C. This is similar to Agost impact layer behaviour, but with no evident indications of goethite or haematite. Thermomagnetic curve for Caravaca Fe-O concretions (Figure 8F) shows no clear signal from original magnetic phases, but the creation of a new, more magnetic phase when heating above 450º C and up to ~525º C; the magnetization of this new phase falls to zero at 600º C in the heating curve, and the cooling curve indicate instead a stable Curie temperature around 500º C. Therefore, the thermomagnetic curve seems to be dominated by the creation of a ferromagnetic low coercivity phase (the external magnetic field during the experiment was 75 mT) from original Fe-bearing paramagnetic phases, somehow similar to the case of Agost magnetic extraction (hand magnet) but with a lower Curie temperature (compare to Figure 4F). The presence of these Fe-O concretions could explain part, but not all, of the impact layer thermomagnetic behaviour (mainly the irreversible character and the creation of the new phase). Values of χ and IRM_{500mT} for Caravaca Fe-O concretions are written down in Table 1: they have higher coercivities than the impact layer bulk sample, but much higher IRM_{500mT}. Therefore, they must contribute significantly to the magnetic characteristics of the impact layer, but there are still very important differences regarding the coercivity distributions and the thermomagnetic behaviour that makes it impossible to explain the impact layer magnetic behaviour as a mere dilution of these Fe-O concretions in a less magnetic matrix.
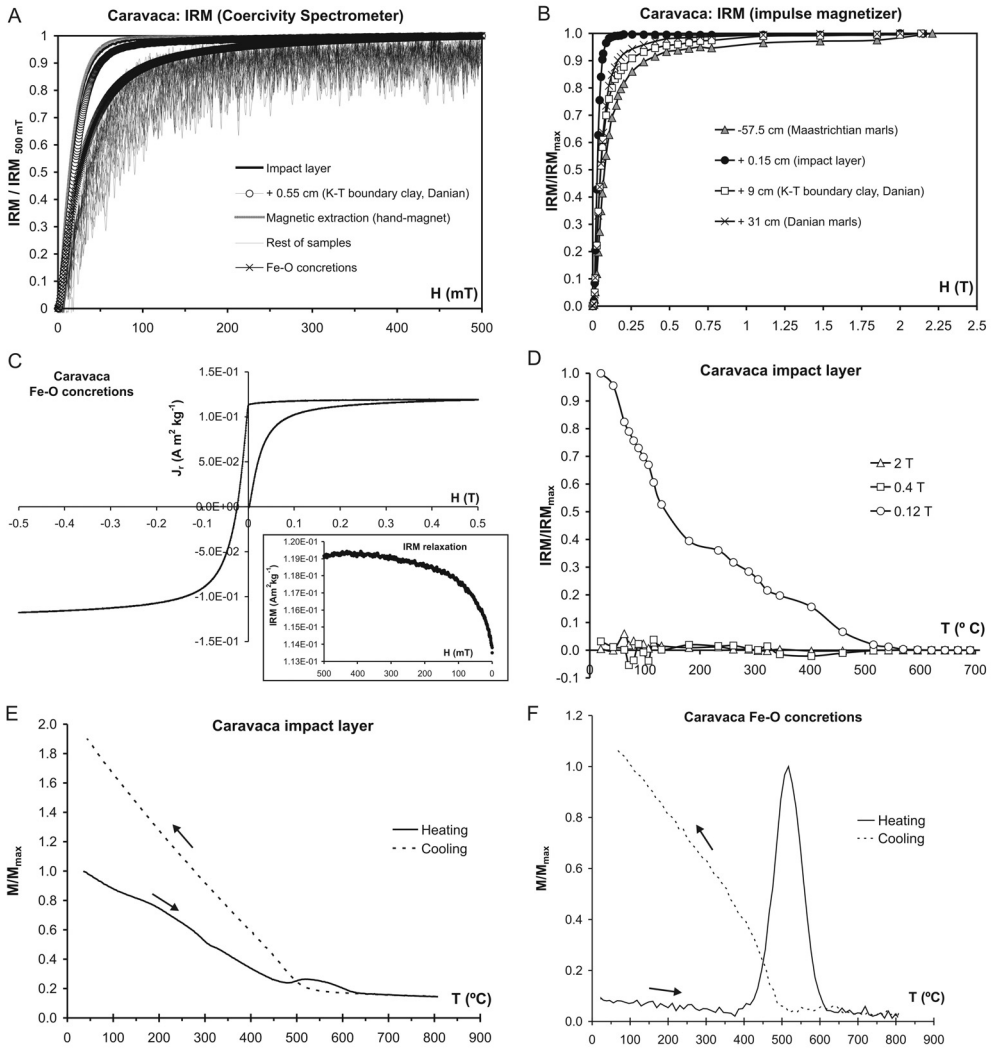
Figure 8. A) IRM back-demagnetization curves (rescaled and normalized) for Caravaca samples, Coercivity Spectrometer up to 0.5 T. B) IRM curves, impulse magnetizer up to > 2 T. C) IRM acquisition and back-demagnetization curve for Caravaca Fe-O concretions; inset, IRM relaxation in the $H_{max}>H>0$ branch. D) 3-axis IRM thermal demagnetization for Caravaca impact layer. E) Thermomagnetic curve for Caravaca impact layer (external field = 1 T). F) Thermomagnetic curve for Caravaca Fe-O concretions (external field = 75 mT).

As in the case of Agost, to analyze any paleoenvironmental trend in Caravaca we have re-drawn Figure 7 without the values of the impact layer and the immediately overlying sample, eliminating the magnetic signature of the impact material. The result is shown in Figure 9. The same clear trend in susceptibility is observed: Maastrichtian material shows low susceptibility, the K-T boundary clay is marked by an increase in susceptibility and it decreases in the Danian marls. Low Danian background values seem to be reached again after $\sim$ 50-55 cm and they are clearly lower than Maastrichtian background values. The IRM_{500mT} shows instead higher values within the Danian than in the Maastrichtian, with minor fluctuations. In Caravaca H_{cr} presents a decreasing trend through the boundary and in the Danian marls, with more pronounced fluctuations during the Maastrichtian and K-T boundary clay and much more stable (but decreasing) values during the Danian. S_{100mT} is negatively coupled with H_{cr}. Figure 10 shows χ and IRM_{500mT} in a carbonate free basis, together with non-carbonate fraction (carbonate data from Martínez-Ruiz, 1994). After the carbonate correction the susceptibility increase in the K-T boundary clay and its decrease in the Danian marls are greatly suppressed, indicating that this behaviour was mainly due to carbonate content variation. This is not as clear as in Agost, probably because for Caravaca the carbonate correction is more imperfect (note for example that carbonate content data do not perfectly match lithology for the clay layer, due to the different samplings made for this work and Martínez-Ruiz, 1994). After carbonate correction, average susceptibility background values for the Danian ($1.7\pm0.5\cdot10^{-7}$ m^3kg^{-1}) are slightly higher than for the Maastrichtian ($1.2\pm0.2\cdot10^{-7}$ m^3kg^{-1}). Even more pronounced, background corrected IRM_{500mT} values are clearly higher in the Danian marls ($2.5\pm0.3\cdot10^{-4}$ Am^2kg^{-1}) than in the Maastrichtian ($0.9\pm0.2\cdot10^{-4}$ Am^2kg^{-1}), implicating an increase in the ferromagnetic fraction in the early Danian. Finally, the magnetic spike associated with the impact layer is maintained after carbonate correction.
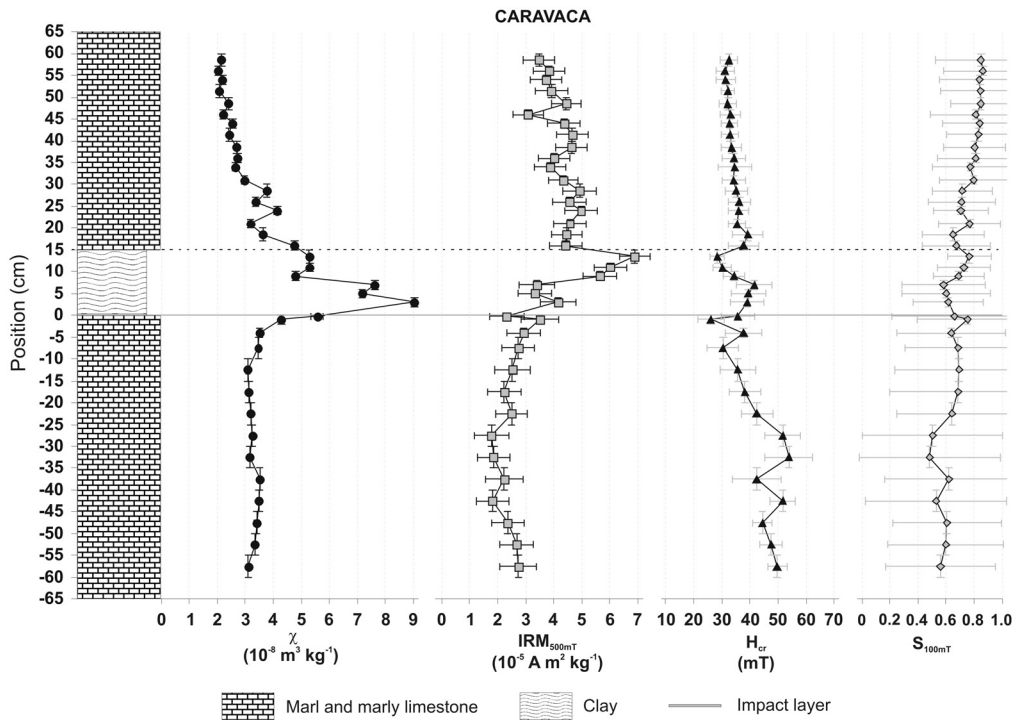
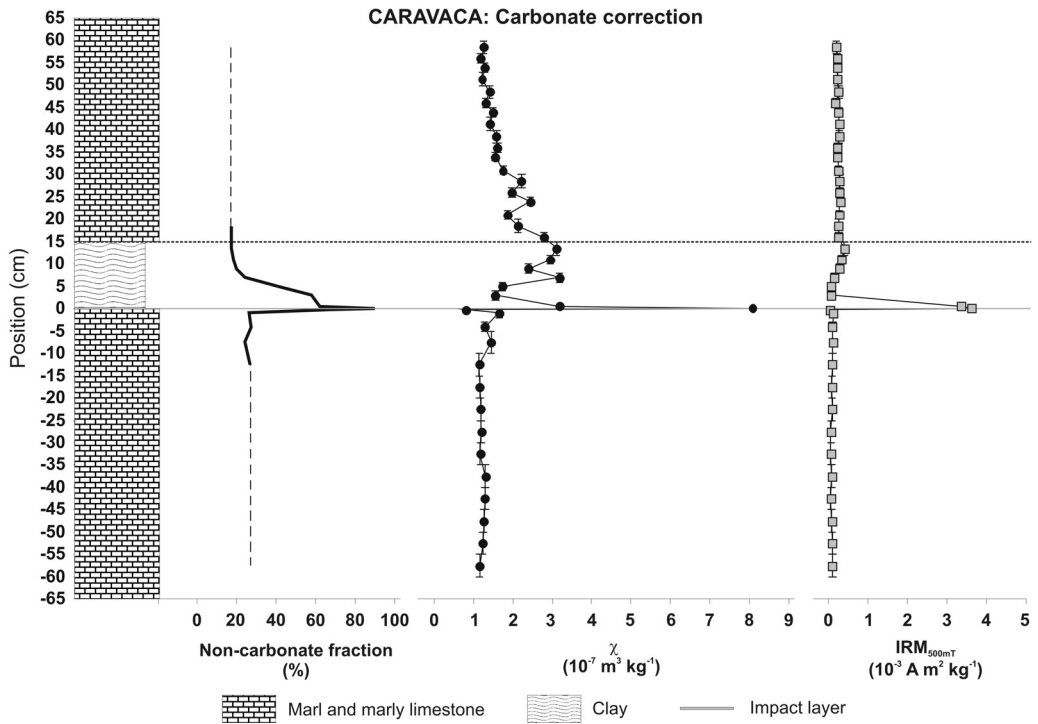**Figure 9.** Caravaca magnetic parameters after eliminating data-points from impact layer and overlying sample.

Figure 10. Caravaca χ and IRM_{500mT} in a carbonate free basis, together with non-carbonate fraction. Dashed line in non-carbonate fraction indicates constant extrapolation of Martínez-Ruiz (1994) data.

The patches of impact layer material in Zumaya show also much higher susceptibility and IRM_{500mT} than Maastrichtian and Danian materials (Figure 11), as well as lower coercivity of remanence and a S_{100mT} ratio closer to 1. IRM curves (Figure 12A) indicate a coercivity distribution displaced to low magnetic fields for the impact layer material. The samples immediately underlying (position -0.25 cm, calcite and clay) and overlying (position +0.3 cm, K-T boundary marly clay) the impact layer show also low coercivities of remanence, S_{100mT} ratios close to 1 and coercivity distributions displaced to low fields. This indicates the presence of the low coercivity phase characteristic of the impact layer in the immediately surrounding material, either as contamination or as original phases. The rest of Maastrichtian and Danian samples show higher coercivities and various contributions of high coercivity phases. In particular, samples of the diagenetically-originated calcite layers at the bottom and at the top of the K-T boundary marly clay present significantly higher coercivities and lower S_{100mT} than the rest, pointing to the presence of authigenically precipitated high-coercivity, antiferromagnetic phases like goethite

or haematite. The thermomagnetic curve for impact layer material (Figure 12B) is dominated by the creation of a new magnetic phase when heating over 475-500º C. The cooling curve shows a Curie temperature around 600º C for this new phase, indicating that magnetite is generated from Fe-bearing phases originally present in the sample, either paramagnetic or ferromagnetic but with lower magnetizations than the resulting magnetite.
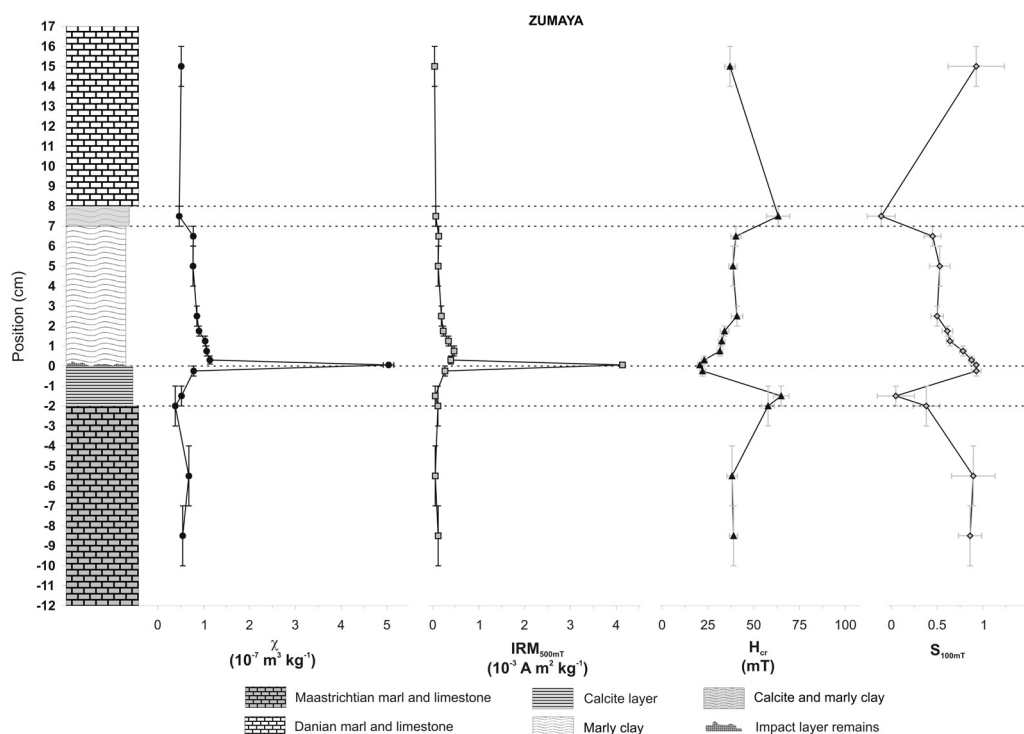

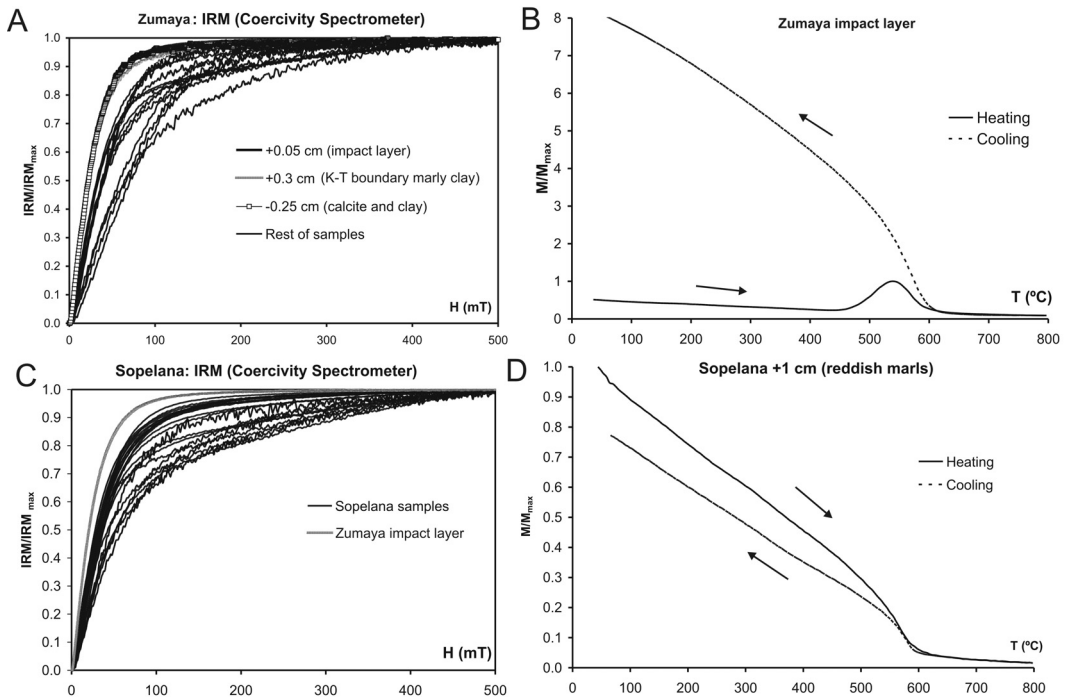**Figure 11.** Zumaya rock magnetic parameters for bulk samples.

Figure 12. A) IRM back-demagnetization curves (rescaled and normalized) for Zumaya samples, Coercivity Spectrometer up to 0.5 T. B) Thermomagnetic curve for Zumaya impact layer (external field = 1 T). C) IRM back-demagnetization curves (rescaled and normalized) for Sopelana samples, Coercivity Spectrometer up to 0.5 T. D) Thermomagnetic curve for Sopelana impact layer (external field = 1 T).

Figure 13 has been constructed after eliminating the impact layer data, to allow a better comparison of magnetic parameters for Maastrichtian and Danian materials. The main changes are connected to the calcite layers, which show low χ and IRM_{500mT}, high H_{cr} and low S_{100mT}, and to the K-T boundary clay, which shows coupled increases in χ and IRM_{500mT} in the initial part and subsequent decreases. Carbonate-free values are plot in Figure 14 (carbonate data from Martínez-Ruiz, 1994). The high K-T boundary marly clay values are greatly suppressed, indicating that the previous changes were due to carbonate fraction changes across the boundary. But the impact layer magnetic spike clearly remains, indicating the presence of a highly magnetic low-coercivity characteristic phase, and not solely a relative increase in ferromagnetic fraction due to carbonate content variations. In Zumaya, our sampling has been too narrow and too sparse to allow a proper investigation of paleoenvironmental magnetic trends similar to Agost and Caravaca; it seems that in Zumaya we have not sampled high enough within the early Danian to reach the new

Danian background values for carbonate fraction. This makes it impossible to ascertain if Zumaya carbonate-fraction trends and their expression through magnetic parameters are similar to those of Agost and Caravaca, which showed an excess carbonate production during the Danian compared to the Maastrichtian, once the background values are recovered. Martínez-Ruiz (1994) carbonate data reached to +28 cm over the boundary, with a non-carbonate fraction of 44% at this position, very close to the average end-Maastrichtian values; it is not known if higher in the stratigraphic column lower background values would be reached, as in Agost and Caravaca.
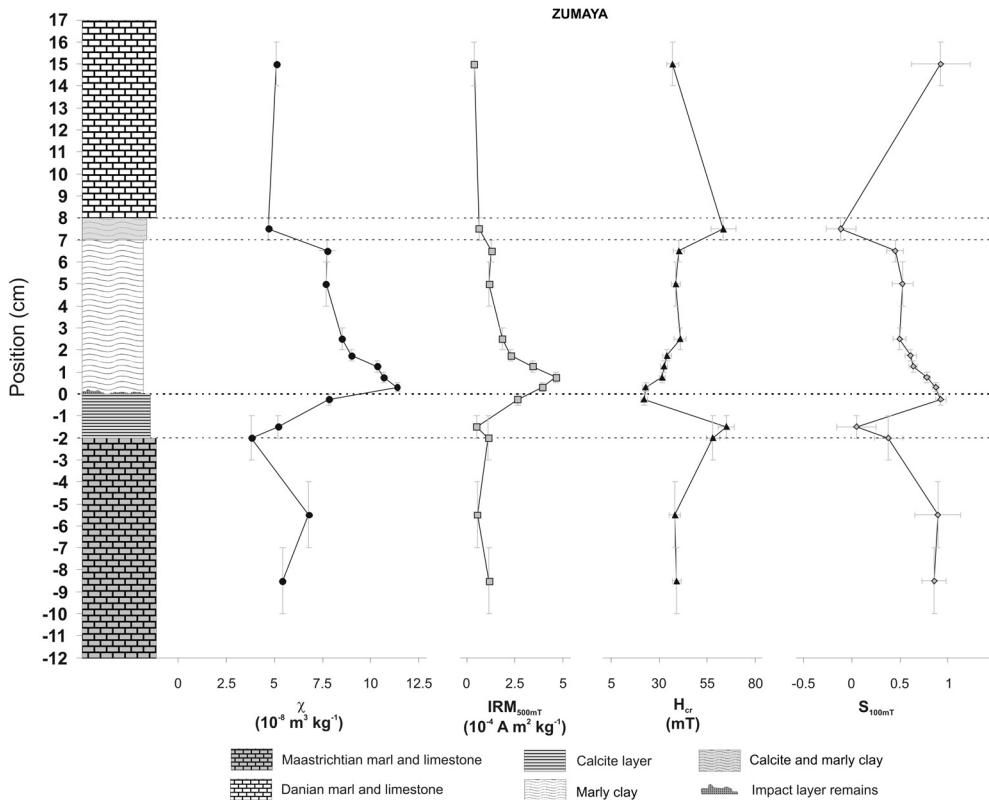

Figure 13. Zumaya magnetic parameters after eliminating data from impact layer.
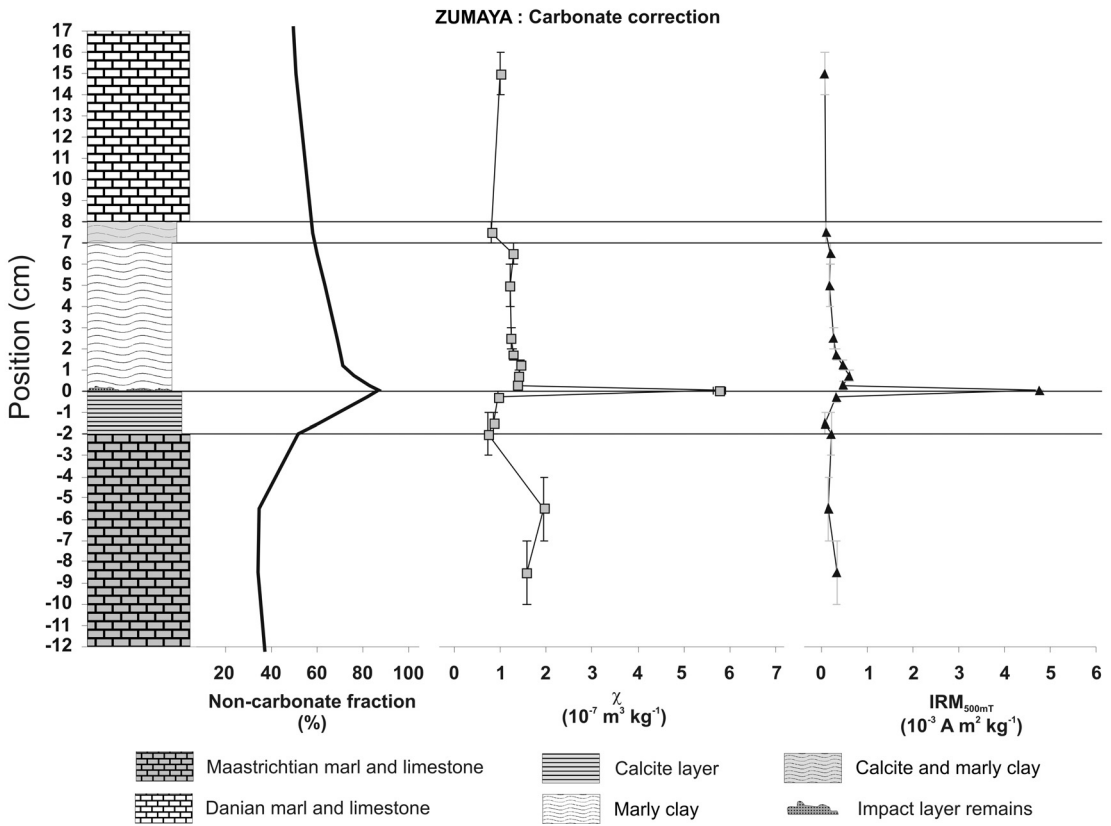
Figure 14. Zumaya χ and IRM_{500mT} in a carbonate free basis, together with non-carbonate fraction.

The stratigraphic variation of magnetic parameters in Sopelana section is plot in Figure 15, and the susceptibility and IRM_{500mT} in a carbonate-free basis together with non-carbonate fraction (Martínez-Ruiz, 1994) are represented in Figure 16. In this case, no evident impact layer was found in the field. Coherently, no magnetic spike is observed in the lower part of the K-T boundary clay-rich interval. Coupled increases in χ and IRM_{500mT} are observed in the clay-rich material, with significant fluctuations. Higher H_{cr} and lower S_{100mT} ratios are detected in Maastrichtian and Danian material, especially in the contact between the clay-rich interval and the overlying Danian limestone. This fact points to the presence of authigenic high-coercivity phases, resulting either from early diagenesis or from weathering, in altered contacts and patches. Sopelana IRM curves (Figure 12C) indicate that all samples have varying contributions from both low and high coercivity phases. They behave similarly to Maastrichtian and Danian samples from the other three studied

sections, and very differently from the impact layer samples (for comparison, Zumaya impact layer curve has also been included in Figure 12C). The reddish marls at the base of the clay-rich interval in Sopelana show a magnetic behaviour not remarkable in any way, with magnetic parameters not different from other clay-rich samples. The thermomagnetic curve (Figure 12D) shows a more or less reversible nature, with a continuous decrease in magnetization up to a maximum Curie point of less than 600º C, indicating the dominance of magnetite-like phases, probably detrital in origin.

Susceptibility and IRM_{500mT} values seem slightly lower in the Danian carbonates than in the end-Maastrichtian, although the sampling is very narrow. This replicates non-carbonate content variation (Figure 16), indicating an excess carbonate production in the early Danian compared to the end-Maastrichtian, as was clearly seen in the case of Agost and Caravaca sections.
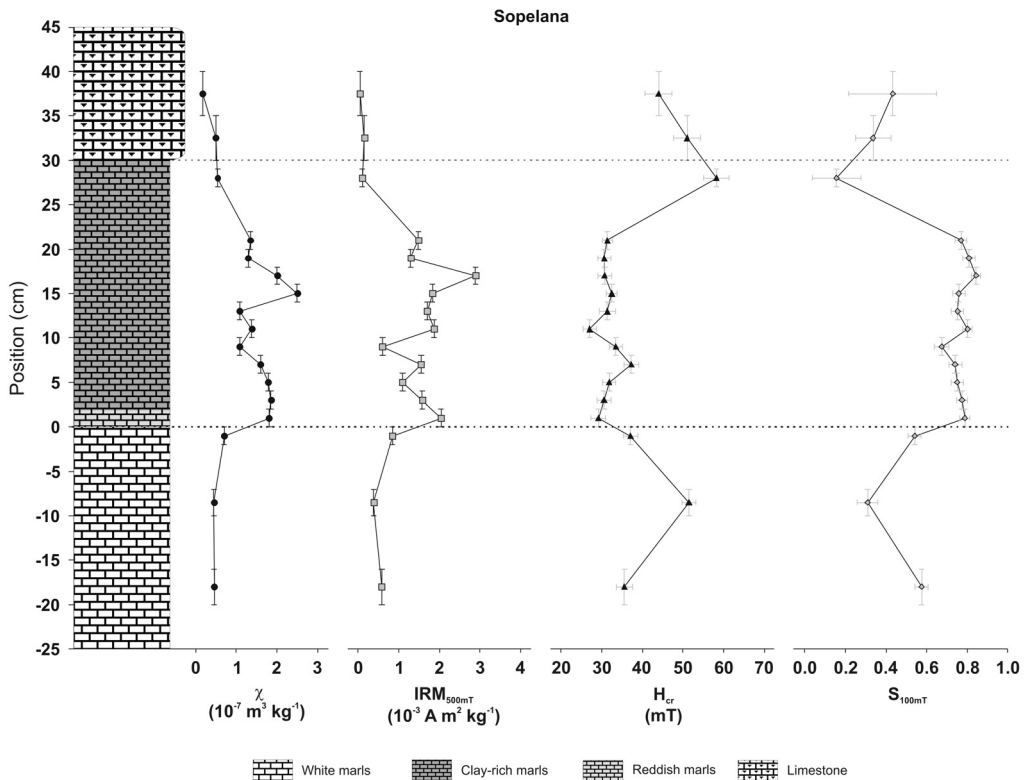

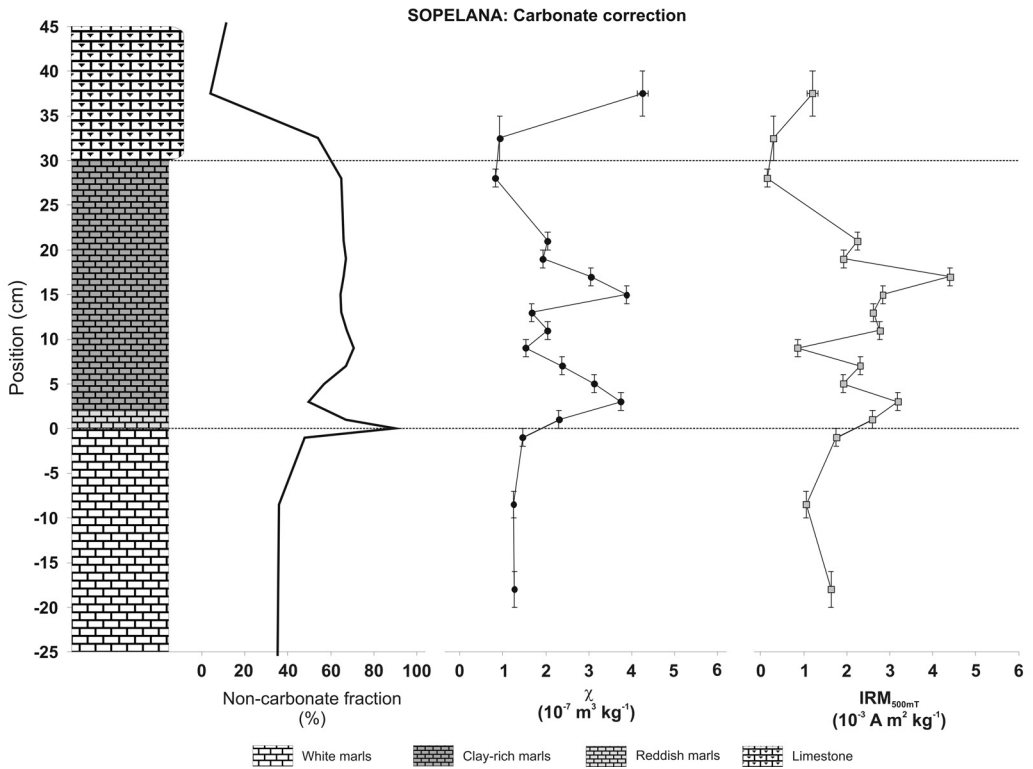**Figure 15.** Sopelana rock magnetic parameters for bulk samples.

Figure 16. Sopelana χ and IRM_{500mT} in a carbonate free basis, together with non-carbonate fraction.

Once the results for the four studied sections have been exposed separately, it would be very useful to compare the magnetic behaviour of impact layer material in all the different sections. Table 1 summarizes the main magnetic parameters, both for bulk impact layer samples, Agost Fe-O microspherules, Caravaca Fe-O concretions and magnetic extractions. Apart from χ, IRM_{500mT}, H_{cr} and S_{100mT} (with their corresponding errors), four additional parameters are tabulated and defined to characterize the relaxation and the coercivity distributions of the IRM. As was stated in the Methodology, coercivity distributions were analyzed with CODICA and GECA programs (Egli, 2004 a, b; Egli, 2005). To properly see what this software performs, Figure 17 presents the results of the coercivity analysis for two different samples, the Caravaca magnetic extraction (hand magnet) and the Agost Fe-O microspherules. CODICA software perform an excellent fit of the original IRM data and greatly reduces the effect of high frequency instrumental noise, as can be seen when comparing the distribution calculated by linearly differentiating the original data and the one calculated by CODICA from the clean fitted IRM curve. From the

CODICA clean coercivity distributions, the parameter H_{peak} has been calculated as the magnetic field where the low-field maximum coercivity distribution value is reached, that is to say, the point where the IRM derivative is maximum. The Caravaca magnetic extraction sample in Figure 17 can be appropriately modelized by GECA with just one SGG component. Agost Fe-O spherules modelization needs instead two components, one with low coercivities and a second with significantly higher coercivities. In Table 1, MAF and DP parameters of GECA fitted components are shown just for the low field components, even for the samples that required two.

Table 1. Magnetic parameters for impact layer samples, Fe-O microspherules and magnetic extractions.

Sample	χ (m^{3}kg^{-1})	IRM$_{500mT}$ (Am^{2}kg^{-1})	H$_{cr}$ (mT)	S$_{100mT}$	δM (%)[a]	H$_{peak}$ (mT)[b]	MAF (mT)	DP (mT)
Caravaca	$7.27 \cdot 10^{-7}$ $\pm 2 \cdot 10^{-9}$	$3.28 \cdot 10^{-3}$ $\pm 1 \cdot 10^{-5}$	14.3 ± 1.5	0.99 ± 0.01	0	18	13	10
Caravaca mag. (1)	$1.14 \cdot 10^{-6}$ $\pm 7 \cdot 10^{-8}$	$4.727 \cdot 10^{-2}$ $\pm 2 \cdot 10^{-5}$	13.6 ± 1.5	0.993 ± 0.002	0	18	13	8
Caravaca Fe-O concretions	$3 \cdot 10^{-7}$ $\pm 1 \cdot 10^{-7}$	$1.19 \cdot 10^{-1}$ $\pm 2 \cdot 10^{-3}$	25 ± 2	0.76 ± 0.02	4	26	26	19
Agost	$6.420 \cdot 10^{-7}$ $\pm 8 \cdot 10^{-10}$	$3.50 \cdot 10^{-3}$ $\pm 1 \cdot 10^{-5}$	16.8 ± 1.4	0.95 ± 0.01	0	25	15	10
Agost mag. (1)	$6.2 \cdot 10^{-7}$ $\pm 1 \cdot 10^{-8}$	$2.56 \cdot 10^{-3}$ $\pm 3 \cdot 10^{-5}$	17 ± 2	0.74 ± 0.02	5	16	16	9
Agost mag. (2)	$1.5 \cdot 10^{-7}$ $\pm 1 \cdot 10^{-8}$ *	$6.5 \cdot 10^{-4}$ $\pm 1 \cdot 10^{-5}$	25 ± 2	0.44 ± 0.03	0	16	14	10
Agost Fe-O spherules	$5.1 \cdot 10^{-7}$ $\pm 1 \cdot 10^{-8}$	$1.29 \cdot 10^{-3}$ $\pm 4 \cdot 10^{-5}$	32 $\pm$ 2	0.28 ± 0.02	10	17	17	9
Zumaya	$5.0 \cdot 10^{-7}$ $\pm 1 \cdot 10^{-8}$	$4.134 \cdot 10^{-3}$ $\pm 3 \cdot 10^{-6}$	20.6 ± 1.4	0.93 ± 0.01	0	24	20	13

(1) Magnetic extraction, hand-magnet

(2) Magnetic extraction, peristaltic pump

(^{a}) This IRM relaxation parameter is defined as $\delta M = 100 \cdot (IRM_{500mT} - IRM_{0mT})/IRM_{500mT}$, that is to say, the difference in % between IRM_{500mT} and the IRM left after decreasing the applied field from 500 to 0 mT (~ 6 minutes).

(^{b}) H_{peak} is the magnetic field corresponding to the relative maximum of the coercivity distribution at low fields (low-coercivity component), as modelled with CODICA.

(*) Calculated from the initial part of the hysteresis cycle, not directly measured.
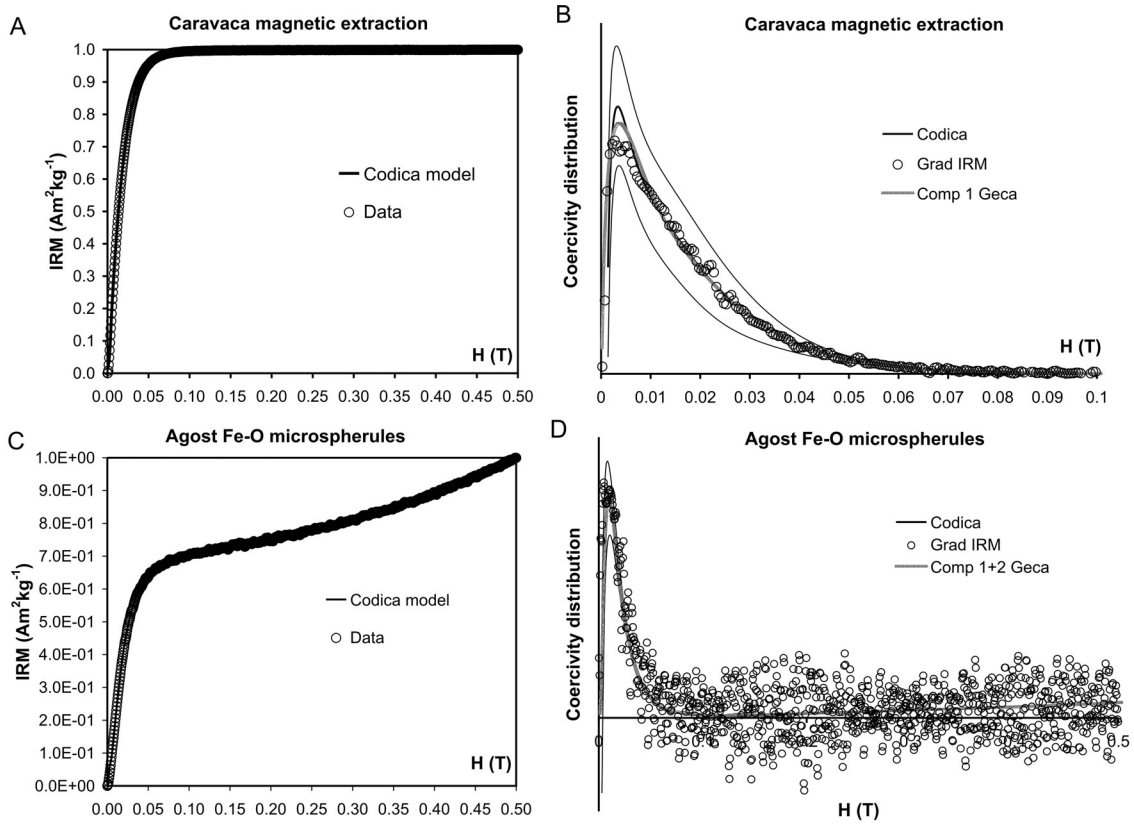
Figure 17. A) Caravaca magnetic extraction (hand magnet) normalized IRM data and CODICA model. B) Comparison of coercivity distributions deduced from data linear numerical gradient, CODICA model and GECA component analysis for Caravaca magnetic extraction. C) Agost Fe-O microspherules normalized IRM data and CODICA model. D) Comparison of coercivity distributions deduced from data linear numerical gradient, CODICA model and GECA component analysis for Agost Fe-O microspherules.

In addition to Table 1, IRM curves for all the impact layer samples, the Agost Fe-O microspherules and the magnetic extractions are shown in Figure 18A. Figure 18B presents a Day-plot for all these samples, where the boundaries of the magnetic-domain regions and the single domain-multi domain mixing curves are all from Dunlop (2002 a, b) and where M_s and H_c parameters have been calculated after correcting the corresponding hysteresis cycles fro the paramagnetic contributions.

The impact layer samples have low coercivities of remanence, between 14 and 20 mT. The higher corresponds to Zumaya. Hand-magnet extractions in Agost and Caravaca show similar results, indicating that the characteristic low coercivity ma-

terial in the impact layer has been at least partially recovered with the magnetic extraction. Agost Fe-O microspherules and peristaltic-pump magnetic extraction behave different, with a low coercivity component and a high coercivity contribution. But the H_{peak}, MAF and DP of the low coercivity component are really close to the same parameters for the impact layer samples, indicating that a significant fraction of the characteristic low coercivity component is included in the Fe-O spherules, and that the peristaltic-pump procedure has separated mainly Fe-O spherules and spherule fragments. Caravaca Fe-O concretions are clearly distinct, with higher coercivities and a coercivity distribution that can be modelled with a main low coercivity component and a secondary high coercivity contribution, the main component being displaced to higher fields than the characteristic impact layer low coercivity material. This agrees with a different origin, proposed to be authigenic by Martínez-Ruiz (1994), who informed that the Caravaca Fe-O concretions are oxidized pyrite clumps. The slightly higher values of H_{cr}, H_{peak} and MAF for Zumaya impact layer, when compared to Agost and Caravaca, are probably due to the low preservation and fragmentary state of the impact layer in the former section, which probably means that the impact layer sample is mixed with more spurious material and possibly with authigenic high coercivity phases precipitated in the bottom calcite slickenside.

Finally, in the Day-plot all the samples fall along curves 1 and 2 of Dunlop (2002 a, b), except Agost Fe-O spherules and Agost peristaltic-pump magnetic extraction, which are displaced upwards and to the right, due to their content in high coercivity material. Curves 1 and 2 correspond to mixtures of a SD and a MD magnetite end-members: SD magnetite with mean sizes of 0.11 microns and MD magnetite with sizes of 131 microns, for curve 1; theoretical SD magnetite grains and 21 microns MD magnetite grains, for curve 2. All the impact layer samples fall in a region where more than 75% multi-domain material is expected for magnetite and magnetite-like low-coercivity minerals.
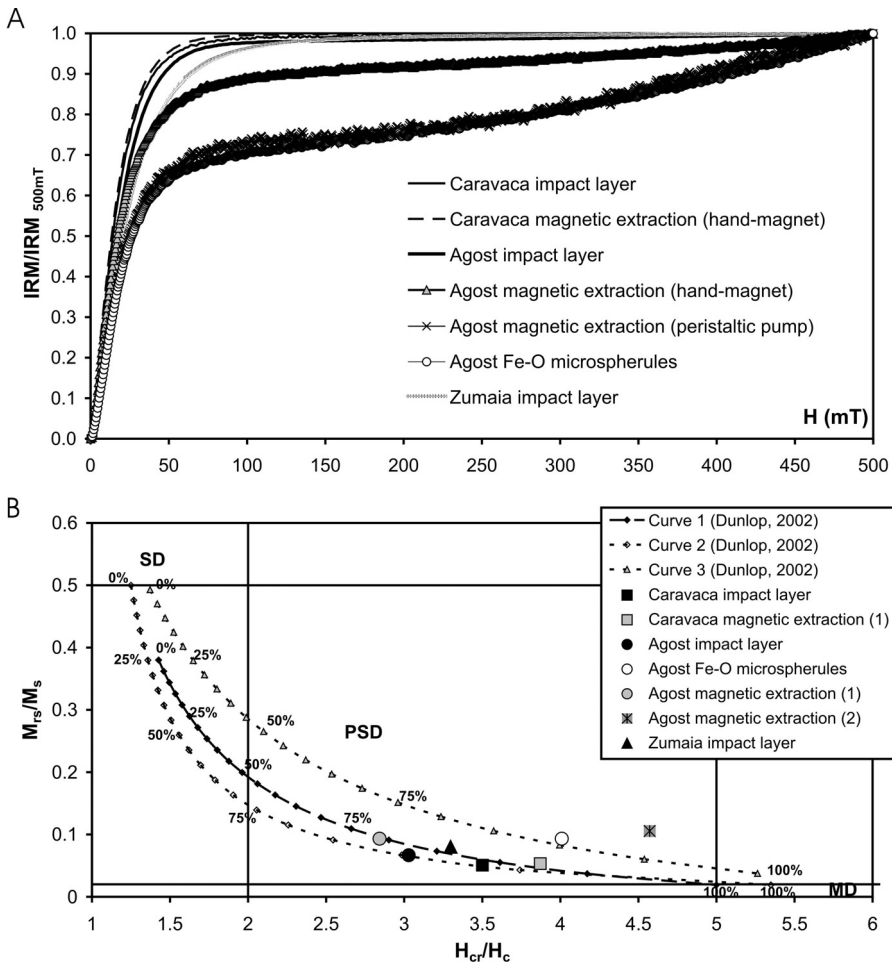
Figure 18. A) IRM back-demagnetization curves (rescaled and normalized) for impact layer samples, microspherules and magnetic extractions (Caravaca, Agost and Zumaya). B) Dayplot for impact layer samples, Fe-O microspherules and magnetic extractions; curves 1, 2 and 3 (Dunlop, 2002 a, b) correspond to mixtures of different SD and MD end-members, with % indicating the fraction of MD material in each case; boundaries for SD, PSD and MD regions are from Dunlop (2002 a, b).

5. DISCUSSION AND CONCLUSIONS

The rock magnetic analysis reveal that the preserved impact layer material and its magnetic extractions are dominated by a distinct ferromagnetic phase with relatively high susceptibility and IRM, with very low coercivity of remanence, low H_{peak} and MAF and a predominantly multi-domain behaviour. It also shows a wide range of IRM unblocking temperatures below 450-500º C and irreversible thermo-

magnetic curves that indicate transformation or Curie temperatures always below 600º C and ranging to low values. To this we must add the absence of Verwey transition as revealed by zero field cooling low-temperature experiments (Villasante-Marcos et al., 2007). This phase, although it seems to be present also in Agost Fe-O microspherules, must be mainly dispersed in the fine clayey matrix material of the impact layer.

This low coercivity phase appears in the impact layer and within the directly contiguous material in Caravaca, Agost and Zumaya, indicating either contamination of contiguous samples with impact layer material during sample preparation or original presence of the distinct phase in a slightly wider stratigraphic range. In Agost, some indications of this material appear also in the last Maastrichtian marls and in K-T boundary clay samples separated in the field and not directly in contact with the impact layer, but located up to 3 cm below and above the impact layer. In this case, contamination seems unlikely and it must strengthened the possibility of this distinct phase being originally distributed in the first centimetres of the Danian and last centimetres of Maastrichtian material. In the Danian case, this could point to a long residence time of this phase in the atmosphere-ocean system, a continuous transportation of this phase from land to the ocean by rivers during some time after the K-T boundary impact, a remobilization of impact layer material by bioturbation or a combination of the three possibilities. In the case of Maastrichtian material, the most plausible explanation seems to be redistribution of impact material by bioturbation, in agreement with the detailed ichnological and bioturbation studies of Rodríguez-Tovar (2005), Rodríguez-Tovar&Uchman (2006) and Rodríguez-Tovar et al. (2006).

All the above-summarized magnetic characteristics are satisfied by Mg, Ni-rich spinels or magnesioferrites, with varying degrees of cation substitution and high oxidation states. Cation substitution in magnetite-like phases, especially by Mg, Al and Cr, serves to decrease Curie temperatures (Nagata, 1953). More importantly, high oxidation states (maghemitization) suppress the Verwey transition of magnetite (see for example Dunlop&Özdemir, 1997) and also introduce phase instability under heating, making the thermomagnetic curves irreversible. As concluded previously for Agost and Caravaca (Villasante-Marcos et al., 2007) and for Petriccio in Italy (Worm&Banerjee, 1987; Cisowski, 1988, 1990), identification of Mg, Ni-rich spinels of meteoritic origin as the distinct magnetic phase in the impact layer is the most plausible possibility. Their multi-domain character is also expected from the reported sizes (Smit&Kyte 1984; Kyte&Smit 1986; Bohor et al., 1986; Robin et al., 1991; Robin et al. 1992; Kyte&Bostwick 1995; Rocchia et al., 1996; Robin&Rocchia, 1998).

Apart from the distinct low coercivity phase, important contributions from high coercivity, antiferromagnetic phases are found in Agost impact layer, Agost Fe-O spherules, Caravaca Fe-O concretions and less pronounced in Zumaya impact layer. In the case of Agost spherules and Caravaca concretions, this high coercivity contribution shows a significant relaxation of the IRM, pointing to a noticeably superparamagnetic fraction and thus very fine grain sizes. These phases can be identified

by means of IRM thermal demagnetization and thermomagnetic curves as a mixture of goethite and haematite, with some X-ray diffraction results (Villasante-Marcos et al., 2007) indicating a dominance of goethite at least in Agost Fe-O spherules. The association of these antiferromagnetic phases with diagenetic alteration is supported by their dominant presence either in totally authigenic precipitates (Caravaca Fe-O concretions, coming from oxidized pyrite framboids) or in diagenetically altered phases (Agost Fe-O spherules, which are microkrystites that have suffered almost total replacement of original material by authigenic minerales, although original textures have been preserved). In the case of Zumaya, the impact layer is poorly preserved and it is associated with an authigenic calcite layer where the presence of high-coercivity material is evident from the magnetic parameters. The interpretation of these high coercivity phases needs to take into account the results found in other sections at proximal (El Mimbral and La Lajilla, NE Mexico) and intermediate (Blake Nose, ODP 1049A, NW Atlantic) distances to Chicxulub. There, Villasante-Marcos et al. (2007) identified distinct thin layers dominated by fine grained goethite and haematite with high superparamagnetic fraction. They were placed on top of the siliciclastic sediments remobilized and deposited by the impact event close to the impact point (Mexican sections) and on top of the slumped spherulitic bed coming from the target material at intermediate distance (Blake Nose). Detailed magnetic and geochemical measurements indicate that these goethite-rich layers are not coupled with iridium anomalies and are related to early-digenesis remobilization of elements.

The high coercivity phases identified by rock magnetism in this work and in Villasante-Marcos et al. (2007) are probably related to those reported by Wdowiak et al. (2001), Verma et al. (2001) and Bhandari et al. (2002) from their Mössbauer spectroscopic analysis, although these works did not report precise descriptions of the proximal sections or of the stratigraphic levels at which their samples were taken, therefore placing some doubts on the inter-comparison of results. The interpretation that our data support is different from that of the previous authors: there is clear evidence that the high coercivity antiferromagnetic phases are not original, but early-diagenetic products. This is in agreement with the results found by Brooks et al. (1985) at Woodside Creek (New Zealand, South Island) by their Mössbauer, X-ray diffraction and geochemical analysis. They identified various antiferromagnetic phases (goethite and haematite) and deduced a purely diagenetic origin. Their model to explain the presence of these phases in the impact layer is similar to that of Montanari (1991), who intensively studied the impact layer at several K-T boundary sections in Italy and examined various types of spherules, including Fe-O microspherules. The results reported in the present paper lead us to essentially the same model: the consequences of the meteoritic impact at the K-T boundary included mass mortality in the pelagic ecosystems, producing a sudden influx of dead organic matter to the water-sediment interphase. This in turn caused anomalous reducing conditions in the sediment, with rapid consumption of interstitial oxygen by the degradation of organic matter mediated by the infaunal benthos, which was less affected by the extinction. Depending on local constrains, conditions differed,

but in general reducing conditions promoted Fe^{2+} mobilization, even pyrite precipitation when sulphate reduction developed. After the extinction, ocean primary productivity collapsed, carbonate production was greatly reduced and therefore both carbonate and organic matter transportation to the bottom decreased. This would drive to a reestablishment of more oxidative conditions in the upper sediment layers, in a similar way to a deepening redox front (see for example Sahota et al., 1995). This would also lead to a re-oxidation of the Fe^{2+} present either in reduced precipitated mineral phases, as pyrite, in the most reducing settings (for example Caravaca and its Fe-O concretions) or present in dissolution within interstitial water, causing precipitation of new authigenic Fe^{3+} oxides-oxyhydroxides, which could contribute to replacement of original impact-related material. Although ferrihydrite (often called amorphous Fe oxide) has long been considered the main Fe^{3+} mineral that will precipitate under oxidation at marine-sediment early-diagenetic redox fronts, it has been recently discovered that direct precipitation of very fine-grained (nanophase) goethite occurs in these processes in a wide variety of marine and lacustrine sedimentary environments (van der Zee et al., 2003). If ferrihydrite was the main precipitate, a progressive transformation to goethite and to more crystalline haematite could be expected under low-temperature oxidative conditions. If fine grained goethite was the precipitated mineral, a similar increase in crystallinity and a transformation to haematite would be also expected (see for example Cornell&Schwertmann, 2003). In any case, the impact layer high coercivity antiferromagnetic phases, dominated by fine grained goethite with a significant superparamagnetic fraction and also with haematite, are very well explained by this early-diagenesis model, which explains also many other characteristics of the mineralogical and geochemical fingerprints of the K-T boundary impact layer. According to this view, the K-T boundary impact layer, 65 Ma after its deposition, retains the magnetic fingerprints both of ferrimagnetic meteoritic impact phases (Mg, Ni-rich spinels) and of antiferromagnetic authigenic phases (fine-grained goethite and haematite) precipitated in a very singular case of non-steady state early diagenesis.

Some remarks should be made regarding the paleoenvironmental sedimentary trends revealed by rock magnetic measurements in Agost and Caravaca when the impact layer signal is eliminated. Susceptibility reflects the contributions of all the minerals in the sample, either if they are diamagnetic (for example calcite), paramagnetic (clays) or ferromagnetic (many iron oxides). It is strongly correlated in both sections with non-carbonate content. This is typical in sediments where detrital ferromagnetic and/or paramagnetic phases account for most of the magnetic fraction. Since calcite has negative susceptibility and because mass normalized susceptibility is being considered, χ variations reflect variations in the terrigenous/carbonate ratio. In Agost and Caravaca, K-T boundary clay shows an increase in non-carbonate fraction and thus in χ, subsequently decreasing in the upper part of the clays and in the first Danian marls until reaching again background values. Lower background values of both χ and non-carbonate fraction in the early Danian indicate the onset of excess carbonate production when compared to the end-Maastrichtian. This means that the environmental effects of the K-T boundary

impact produced in the first place a widespread productivity collapse and an associated pronounced fall in carbonate deposition, which resulted in the K-T boundary clay. Later, paralleling the recovery of productivity in pelagic ecosystems, carbonate production resumed and reached even more vigorous rates than during the end-Maastrichtian, an excess carbonate production. The stratigraphic interval spanned by the K-T boundary clays and the first Danian marls until the background values are again recovered is around 45 cm in Agost and 50-55 cm in Caravaca. A gross estimation of the temporal equivalent can be intended based on mean compacted sedimentation rates deduced from biostratigraphy and magnetostratigraphy. For Caravaca there are two main sedimentation rate estimations: Smit (1990) reports ~2 cm/ka in the lower Danian; Arinobu et al. (1999) took into account the lower carbonate content of the clay layer and, assuming a constant rate of terrigenous discharge, reported 0.8 cm/ka for the K-T boundary clay and 1.7 cm/ka for the early Danian marls. This would translate to ~25 ka (Smit, 1990) and ~40 ka (Arinobu et al., 1999) between the K-T impact and the onset of excess carbonate production, the second figure being probably more precise. Groot et al. (1989) estimated an average compacted sedimentation rate of 0.83 cm/ka for Agost during the early Danian. This would translate to ~54 ka between the meteoritic impact and the onset of excess carbonate production. We can try a better estimation following Arinobu et al. (1999) and recalculating a more precise sedimentation rate for the clay layer, assuming that the rate of terrigenous material accumulation was constant through the boundary and that the fall in carbonate production resulted in lower total sedimentation rates. Since mean carbonate content is around 33.1 % in the clay layer and 83.4 % in the first meter of Danian marls, it would imply that sedimentation rates in the clay layer are around 2.5 times lower than in the Danian marls. Assuming 0.83 cm/ka for the marls, a new figure of ~0.33 cm/ka for the clays is obtained. With these new rates, the temporal separation between impact and the onset of excess carbonate production in Agost is estimated in ~75 ka. Caravaca and Agost figures are different by a factor of ~2, but we have to consider that these are only very gross estimations.

Although our sampling in Sopelana was much narrower, carbonate and susceptibility data point to a recovery of carbonate production ~40 cm above the boundary. Mary et al. (1991) reported magnetostratigraphic data for Sopelana section, calculating an average compacted sedimentation rate of 0.7 cm/ka for the Danian part of the section. Following this, the above mentioned 40 cm would translate to ~57 ka between K-T boundary impact and onset of excess carbonate production. Considering the grossness of the estimations, and that Sopelana is in a completely different paleogeographic region, the overall coincidence with Caravaca and Agost results is remarkable, strengthening the conclusion that carbonate production seems to have recovered in a period somewhere between 40 and 75 ka after the impact.

Finally, in Agost and Caravaca the early Danian seems to be associated to higher susceptibilities and IRM_{500mT}, in a carbonate-free basis, than the end-Maastrichtian, indicating an increase of ferromagnetic content in the non-carbonate fraction of Danian sediments. In Agost, this is connected to appreciable fluctuations, and in

Caravaca it seems to be related to a decreasing trend in the coercivity of remanence. No detailed explanation can be proposed without additional data, but it seems that the K-T impact provoked paleoenvironmental and climatic perturbations that affected both the terrigenous/carbonate ratio and the ferromagnetic input to the sediments, either terrigenous- or authigenically-derived. This could be connected to the reported increase in continental weathering across the boundary as deduced from strontium isotopes (MacLeod et al., 2001). We could even consider a possible link between the onset of excess carbonate production and the increase in ferromagnetic input in the early Danian, may be due to enhanced ocean fertilization by land-derived material enriched in Fe-bearing minerals and the opportunistic response of a recovering biota. Obviously, this is just a suggestion without firm support by the presented data.

6. ACKNOWLEDGEMENTS

7. REFERENCES

ALVAREZ, L.W., W. ALVAREZ, F. ASARO & H.V. MICHEL (1980). Extraterrestrial cause for the Cretaceous-Tertiary extinction. *Science* 208, 1095-1108.

ARENILLAS, I., J.A. ARZ, J.M. GRAJALES-NISHIMURA, G. MURILLO-MUÑETÓN, W. ALVAREZ, A. CAMARGO-ZANOGUERA, E. MOLINA & C. ROSALES-DOMÍNGUEZ, (2006). Chicxulub impact event is Cretaceous/Paleogene boundary in age: New micropaleontological evidence. *Earth and Planetary Science Letters* 249, 241-257.

ARINOBU, T., R. ISHIWATARI, K. KAIHO & M.A. LAMOLDA (1999). Spike of pyro-synthetic polycyclic aromatic hydrocarbons asssocaited with an abrupt decrease in d13C of a terrestrial biomarker at the Cretaceous-Tertiary boundary at Caravaca, Spain. *Geology* 27, 723-726.

ARZ, J.A., L. ALEGRET & I. ARENILLAS, I. (2004). Foraminiferal biostratigraphy and paleoenvironmental reconstruction at the Yaxcopoil-1 drill hole (Chicxulub crater, Yucatán Peninsula). *Meteoritics and Planetary Science* 39, 1099-1111.

BACETA, J.I. & V. PUJALTE. Lithostratigraphy of the K/P boundary interval. In G. Bernaola, J.I. Baceta, A. Payros, X. Orue-Etxebarria & E. Apellaniz (EDS.). *The Paleocene and Lower Eocene of the Zumaia section (Basque Basin). Field Trip Guidebook.* Climate&Biota of the Early Paleogene 2006 Post-Conference Field Excursion Guidebook, Bilbao, Spain, 82 pp.

BHANDARI, N., H.C. VERMA, C. UPADHYAY, A. TRIPATHI & R.P. TRIPATHI (2002). Global occurrence of magnetic and superparamagnetic iron phases in Cretaceous-Tertiary boundary clays. In C. Koeberl & K.G. MacLeod (eds.). *Catastrophic events and*

mass extinctions: impacts and beyond. *Geological Society of America Special Paper* 356, 201-211.

BOHOR, B.F., E.E. FOORD, P.J. MODRESKI & D.M. TRIPLEHORN (1984). Mineralogic evidence for an impact event at the Cretaceous-Tertiary event. *Science* 224, 867-869.

BOHOR, B.F., E.E. FOORD & R. GANAPATHY (1986). Magnesioferrite from the Cretaceous-Tertiary boundary, Caravaca, Spain. *Earth and Planetary Science Letters* 81, 57-66.

BOHOR, B.F., P.J. MODRESKI & E.E. FOORD (1987). Shocked quartz in the Cretaceous-Tertiary boundary clays: Evidence for a global distribution. *Science* 236, 705-709.

BROOKS, R.R., P.L. HOEK, R.D. REEVES, R.C. WALLACE, J.H. JOHNSTON, D.E. RYAN, J. HOLZBECHER & J.D. COLLEN (1985). Weathered spheroids in a Cretaceous/Tertiary boundary shale at Woodside Creek, New Zealand. *Geology* 13, 738-740.

CANDE, S.C. & D.V. KENT (1995). Revised calibration of the geomagnetic polarity timescale for the Late Cretaceous and Cenozoic. *Journal of Geophysical Research* 100 (B4), 6093–6095.

CISOWSKI, S.M. (1988). Magnetic properties of K/T and E/O microspherules: origin by combustion?. *Earth and Planetary Science Letters* 88, 193-208.

CISOWSKI, S.M. (1990.) The significance of magnetic spheroids and magnesioferrite occurring in K/T boundary sediments. In V.L. Sharpton & P.D. Ward (EDS.). *Global catastrophes in Earth history: An interdisciplinary conference on impacts, volcanism and mass mortality. Geological Society of America Special Paper* 247, 359-365.

CLAEYS, PH., W. KIESSLING & W. ALVAREZ (2002). Distribution of Chicxulub ejecta at the Cretaceous-Tertiary boundary. In C. Koeberl & K.G. MacLeod (eds.). *Catastrophic events and mass extinctions: impacts and beyond. Geological Society of America Special Paper* 356, 55-68.

CORNELL, R.M., U. SCHWERTMANN (2003). *The Iron Oxides*. Wiley-VCH Verlag GmbH & Co., Germany, 664 pp.

D'HONDT, S., J. KING & C. GIBSON (1996). Oscillatory marine response to the Cretaceous-Tertiary impact. *Geology* 24, 611-614.

DUNLOP, D.J. (2002 a). Theory and application of the Day plot (Mrs/Ms versus Hcr/Hc): 1. Theoretical curves and tests using titanomagnetite data. *Journal of Geophysical Research* 107 (B3), EPM 4-1–EPM 4-22.

DUNLOP, D.J. (2002 b). Theory and application of the Day plot (Mrs/Ms versus Hcr/Hc): 2. Application to data for rocks, sediments and soils. *Journal of Geophysical Research* 107 (B3), EPM 5-1–EPM 5-15.

DUNLOP, D.J. & Ö. ÖZDEMIR (1997). *Rock magnetism: fundamentals and frontiers*. Cambridge University Press, Cambridge, UK, 573 pp.

EGLI, R. (2004 a). Characterization of individual rock magnetic components by analysis of remanence curves, 1. Unmixing natural sediments. *Studia Geophysica et Geodaetica*, 48, 391-446.

EGLI, R. (2004 b). Characterization of individual rock magnetic components by analysis of remanence curves, 2. Fundamental properties of coercivity distributions. *Physics and Chemistry of the Earth*, 29, 851-867.

EGLI, R. (2005). *User's guide to the MAG-MIX, magnetic unmixing software packet, Release 1, April 2005*. Freely distributed at
http://dourbes.meteo.be/aarch.net/magmix.man.pdf .

GANAPATHY, R. (1980) A major meteorite impact on the Earth 65 million years ago: Evidence from the Cretaceous-Tertiary boundary clay. *Science* 209, 921-923.

GRISCOM, D.L., V. BELTRAN-LOPEZ, C.I. MERZBACHER & E. BOLDEN (1999). Electron spin resonance of 65-million-year-old glasses and rocks from the Cretaceous-Tertiary boundary. *Journal of Non-crystalline Solids* 253, 1-22.

HILDEBRAND, A.R., G.T. PENFIELD, D.A. KRING, M. PILKINGTON, A. CAMARGO, S.B. JACOBSEN & W.V. BOYNTON (1991). Chicxulub crater: A possible Cretaceous/Tertiary boundary impact crater on the Yucatan Penninsula, Mexico. *Geology* 19, 867-871.

JABLONSKI, D. (1994). Extinctions in the fossil record. *Philosophical Transactions of the Royal Society*, B344, 11-17.

JASONOV, P.G., D.K. NOURGALIEV, B.V. BUROV & F. HELLER (1998). A modernized coercivity spectrometer. *Geologica Carpathica*, 49, 224-225.

KIESSLING, W. & P. CLAEYS (2001). A geographic database approach to the KT boundary. In E. Buffetaut & C. Koeberl (eds.). *Geological and biological effects of impact events.* Springer, Berlin, Germany, 83-140.

KRING, D.A. & W.V. BOYNTON (1992). Petrogenesis of an augite-bearing melt rock in the Chicxulub structure and its relationship to K/T impact spherules in Haiti. *Nature* 358, 141-144.

KROGH, T.E., S.L. KAMO, V.L. SHARPTON, L.E. MARIN & A.R. HILDEBRAND (1993). U-Pb ages of single shocked zircons linking distal K/T ejecta to the Chicxulub crater. *Nature* 366, 731-734.

KYTE, F.T. (2002). Tracers of the extraterrestrial component in sediments and inferences for Earth's accretion history. In C. Koeberl & K.G. MacLeod (eds.). *Catastrophic events and mass extinctions: impacts and beyond. Geological Society of America Special Paper* 356, 21-38.

KYTE, F.T. & J. SMIT (1986). Regional variations in spinel compositions: an important key to the Cretaceous/Tertiary event. *Geology* 14, 485-487.

KYTE, F.T. & J.A. BOSTWICK (1995). Magnesioferrite spinel in Cretaceous/Tertiary boundary sediments of the Pacific basin: Remnants of hot, early ejecta from the Chicxulub impact?. *Earth and Planetary Science Letters* 132, 113-127.

KYTE, F.T., Z. ZHOU & J.T. WASSON (1980). Siderophile-enriched sediments from the Cretaceous-Tertiary boundary. *Nature* 288, 651-656.

LAMOLDA, M.A., X. ORUE-ETXEBERRIA, F. PROTO-DECIMA (1983). The Cretaceous-Tertiary boundary in Sopelana (Biscay, Basque Country). *Zitteliana*, 10, 663-670.

LAPLACE, P.S. (1796). *Exposition du systeme du monde*. Paris. Spanish edition: *Exposicion del sistema del mundo*, 2005, Critica, Barcelona, Spain.

LAUBENFELS, M.W.d. (1956). Dinosaur extinction: One more hypothesis. *Journal of Paleontology* 30, 207-218.

LOWRIE, W. (1990). Identification of ferromagnetic minerals in a rock by coercivity and unblocking temperature properties. *Geophysical Research Letters* 17, 159-162.

LUCK, J.M. & K.K. TUREKIAN (1983). Osmium-187/Osmium-186 in Manganese nodules and the Cretaceous-Tertiary boundary. *Science* 222, 613-615.

MACLEOD, N., P.F. RAWSON, P.L. FOREY, F.T. BANNER, M.K. BOUDHAGER-FADEL, P.R. BOWN, J.A. BURNETT, P. CHAMBERS, S. CULVER, S.E. EVANS, C. JEFFERY, M.A. KAMINSKI, A.R. LORD, A.C. MILNER, A.R. MILNER, N. MORRIS, E. OWEN, B.R. ROSEN, A.B. SMITH, P.D. TAYLOR, E. URQUHART & J.R. YOUNG

(1997). The Cretaceous-Tertiary biotic transition. *Journal of the Geological Society, London* 154, 265-292.

MACLEOD, K.G., B.T. HUBER & P.D. FULLAGAR (2001). Evidence for a small (~0.000030) but resolvable increase in seawater $^{87}Sr/^{86}Sr$ ratios across the Cretaceous-Tertiary boundary. *Geology* 29, 303-306.

MARTIN-ALGARRA, A. & J.A. VERA (2004). La Cordillera Bética y las Baleares en el contexto del Maditerráneo Occidental. In J.A. Vera (ed.). *Geología de España. Instituto Geológico y Minero de España & Sociedad Geológica de España*, Madrid, Spain, 884 pp.

MARTÍNEZ-RUIZ, F. (1994). *Geoquímica y mineralogía del tránsito Cretácico-Terciario en las Cordilleras Béticas y en la Cuenca Vasco-Cantábrica.* Ph. D. Thesis, Universidad de Granada, Spain, 281 pp.

MARTINEZ-RUIZ, F., M. ORTEGA-HUERTAS, I. PALOMO & M. BARBIERI (1992). The geochemistry and mineralogy of the Cretaceous-Tertiary boundary at Agost (southeast Spain). *Chemical Geology* 95, 265-281.

MARTINEZ-RUIZ, F., M. ORTEGA-HUERTAS, I. PALOMO & P. ACQUAFREDDA (1997). Quench textures in altered spherules from the Cretaceous-Tertiary boundary layer at Agost and Caravaca, SE Spain. *Sedimentary Geology* 113, 137-147.

MARTINEZ-RUIZ, F., M. ORTEGA-HUERTAS & I. PALOMO (1999). Positive Eu anomaly development during diagenesis of the K/T boundary ejecta layer in the Agost section (SE Spain): implications for trace-element remobilization. *Terra Nova* 11, 290-296.

MARY, C., M.G. MOREAU, X. ORUE-ETXEBARRIA, E. APELLANIZ & V. COURTILLOT (1991). Biostratigraphy and magnetostratigraphy of the Cretaceous-Tertiary Sopelana section (Basque Country). *Earth and Planetary Science Letters*, 106, 133-150.

MAUPERTUIS, P.L. (1750). *Essai de cosmologie*. Amsterdam. Spanish edition: *El Orden Verosimil del Cosmos*, 1992, Alianza, Madrid, Spain.

MOLINA, E., L. ALEGRET, I. ARENILLAS, J.A. ARZ, N. GALLALA, J. HARDENBOL, K. VON SALIS, E. STEURBAUT, N. VANDENBERGHE & D. ZAGHBIB-TURKI (2006). The Global Boundary Stratotype Section and Point for the base of the Danian Stage (Paleocene, Paleogene, "Tertiary", Cenozoic) at El Kef, Tunisia-Original definition and revision. *Episodes* 29, 263-273.

MONTANARI, A. (1991). Authigenesis of impact spheroids in the K/T boundary clay from Italy: New constraints for high-resolution stratigraphy of terminal Cretaceous events. *Journal of Sedimentary Petrology* 61, 315-339.

MONTANARI, A., R.L. HAY, W. ALVAREZ, F. ASARO, H.V. MICHEL & L.W. ALVAREZ (1983). Spheroids at the Cretaceous-Tertiary boundary are altered impact droplets of basaltic composition. *Geology* 11, 668-671.

MORDEN, S. J. (1993). Magnetic analysis of K/T boundary layer clay froms Stevns Klint, Denmark. *Meteoritics* 28, 595-599.

NAGATA, T. (1953). *Rock magnetism.* Maruzen Company Ltd., Tokyo, Japan, 225 pp.

PENFIELD, G.T. & A. CAMARGO (1981). Definition of a major igneous zone in the central Yucatan platform with aeromagnetics and gravity. *Society of Exploration Geophysicists Technical Program, Abstracts and Bibliographies* 51:37.

QUITTE, G., E. ROBIN, F. CAPMAS, S. LEVASSEUR, R. ROCCHIA, J.L. BIRCK & C. ALLEGRE (2003). Carbonaceous or ordinary chondrite as the impactor at the K/T boundary ? Clues from Os, W and Cr isotopes. *Lunar and Planetary Science Conference XXXIV*, Abstracts, 1615.

QUITTE, G., E. ROBIN, S. LEVASSEUR, F. CAPMAS, R. ROCCHIA, J.L. BIRCK & C.J. ALLEGRE (2007). Osmium, tungsten, and chromium isotopes in sediments and in Ni-rich spinel at the K-T boundary: Signature of a chondritic impactor. *Meteoritics and Planetary Science* 42, 1567-1580.

RAUP, D.M. & J.J. SEPKOSKI Jr. (1982). Mass extinctions in the marine fossil record. *Science* 215, 1501-1503.

REBOLLEDO-VIEYRA, M. & J. URRUTIA-FUCUGAUCHI (2006). Magnetostratigraphy of the Cretaceous/tertiary boundary and early Paleocene sedimentary sequence from the Chicxulub impact crater. *Earth Planets Space* 58, 1309-1314.

ROBIN, E. & R. ROCCHIA (1998). Ni-rich spinel at the Cretaceous-Tertiary boundary of El Kef, Tunisia. *Bulletin de la Société géologique de France* 169, 365-372.

ROBIN, E., D. BOCLET, PH. BONTE, L. FROGET,C. JEHANNO & R. ROCCHIA (1991). The stratigraphic distribution of Ni-rich spinels in Cretaceous-Tertiary boundary rocks at El Kef (Tunisia), Caravaca (Spain) and Hole 761C (Leg 122). *Earth and Planetary Science Letters* 107, 715-721.

ROBIN, E., PH. BONTE, L. FROGET, C. JEHANNO & R. ROCCHIA (1992). Formation of spinels in cosmic objects during atmospheric entry: a clue to the Cretaceous-Tertiary boundary event. *Earth and Planetary Science Letters* 108, 181-190.

ROCCHIA, R., D. BOCLET, P. BONTE, E. BUFFEAUT, X. ORUE-ETXEBERRIA, J. JAEGER, C. JEHANNO (1988). Structure de l'anomalie en iridium a la limite Cretace-Tertiaire du site de Sopelana (Pays basque Espagnol). *Comptes Rendus de l'Academie de Sciences de Paris* 307, 1217-1223.

ROCCHIA, R., E. ROBIN, T. CACHIER, B. LIM, H. LEROUX, E. APELLANIZ & X. ORUE-ETXEBARRIA (1996). Impact remains in K-T boundary sediments from the Basque Country. *Meeting on the Cretaceous-Tertiary boundary: biological and geological aspects*, Paris, France. Abstracts.

RODRÍGUEZ-TOVAR, F.J. (2005). Fe-oxide spherules infilling Thalassinoides burrows at the Cretaceous-Paleogene (K-P) boundary: Evidence of a near-contemporaneous macro-benthic colonization during the K-P event. *Geology* 33, 585-588.

RODRÍGUEZ-TOVAR, F.J. & A. UCHMAN (2006). Ichnological analysis of the Cretaceous-Paleogene boundary interval at the Caravaca section, SE Spain. *Palaeogeography, Palaeoclimatology, Palaeoecology* 242, 313-325.

RODRÍGUEZ-TOVAR, F.J., F. MARTÍNEZ-RUIZ & S.M. BERNASCONI (2006). Use of high-resolution ichnological and stable isotope data for assesing completeness of a K-P boundary section, Agost, Spain. *Palaeogeography, Palaeoclimatology, Palaeoecology* 237, 137-146.

SAHOTA, J.T.S., S.G. ROBINSON & F. OLFIELD (1995). Magnetic measurements used to identify paleoxidation fronts in deep-sea sediments from the Madeira Abyssal Plain. *Geophysical Research Letters* 22, 1961-1964.

SEPKOSKI Jr., J.J. (1996). Patterns of Phanerozoic extinction: A perspective from global data bases. In O. H. Walliser (ed.). *Global events and event stratigraphy in the Phanerozoic*, Springer-Verlag, Berlin, Germany, 35-51.

SEPKOSKI Jr., J.J. (2002). A compendium of Fossil marine animal genera. *Bulletin of the American Paleontological Scociety* 363 (Paleontological Research Institute, Ithaca, New York).

SHARPTON, V.L., D.B. DALRYMPLE, L.E. MARIN, G. RYDER, B.C. SCHURAYTZ & J. URRUTIA-FUCUGAUCHI (1992). New links between the Chicxulub impact structure and the Cretaceous/Tertiary boundary. *Nature* 359, 819-821.

SHUKOLYUKOV, A. & G.W. LUGMAIR (1998). Isotopic evidence for the Cretaceous-Tertiary impactor and its type. *Science* 282, 927-929.

SIGURDSSON, H., P. BONTÉ, L. TURPIN, M. CHAUSSIDON, N. METRICH, M. STEINBERG, P. PRADEL & S. D'HONDT (1991). Geochemical constraints on source region of Cretaceous/Tertiary impact glasses. *Nature* 353, 839-842.

SMIT, J. & J. HERTOGEN (1980). An extraterrestrial event at the Cretaceous-Tertiary boundary. *Nature* 285, 198-200.

SMIT, J. & G. KLAVER (1981). Sanidine spherules at the Cretaceous-Tertiary boundary indicate a large impact event. *Nature* 292, 47-49.

SMIT, J. & F.T. KYTE (1984). Siderophile-rich magnetic spheroids from the Cretaceous-Tertiary boundary in Umbria, Italy. *Nature* 310, 403-405.

SMIT, J., A. MONTANARI, N.H.M. SWINBURNE, W. ALVAREZ, A.R. HILDEBRAND, S.V. MARGOLIS, PH. CLAEYS, W. LOWRIE & F. ASARO (1992). Tektite-bearing, deep-water clastic unit at the Cretaceous-Tertiary boundary in northeastern Mexico. *Geology* 20, 99-103.

SWISHER III, C.C., J.M. GRAJALES-NISHIMURA, A. MONTANARI, S.V. MARGOLIS, P. CLAEYS, W. ALVAREZ, P. RENNE, E. CEDILLO-PARDO, F.J.M.R. MAURRASSE, G.H. CURTIS, J. SMIT & M.O. MCWILLIAMS (1992). Coeval 40Ar/39Ar ages of 65.0 million years ago from Chicxulub crater melt rock and Cretaceous-Tertiary boundary tektites. *Science* 257, 954-958.

TEN KATE, W.G.H.Z. & A. SPRENGER (1993). Orbital cyclicities above and below the Cretaceous/Paleogene boundary at Zumaya (N Spain), Agost and Relleu (SE Spain). *Sedimentary Geology* 87, 69-101.

TRINQUIER, A., J.L. BIRCK & C.J. ALLEGRE (2006). The nature of the K-T impactor. A ^{54}Cr reappraisal. *Earth and Planetary Science Letters* 241, 780-788.

TUREKIAN, K. K. (1982). Potential of ^{187}Os/^{186}Os as a cosmic versus terrestrial indicator in high iridium layers of sedimentary strata. In L.T. Silver & P.H. Schultz (eds.). *Geological implications of impacts and large asteroids and comets on the Earth. Geological Society of America Special Paper* 190, 243-249.

URRUTIA-FUCUGAUCHI, J., L. MARIN & V.L. SHARPTON (1994). Reverse polarity magnetized melt rocks from the Cretacous/Tertiary Chicxulub structure, Yucatan peninsula, Mexico. Tectonophysics 237, 105-112.

VAN DER ZEE, C., D.R. ROBERTS, D.G. RANCOURT & C.P. SLOMP (2003). Nanogoethite is the dominant reactive oxyhydroxide phase in lake and marine sediments. *Geology* 31, 993-996.

VERMA, H.C., C. UPADHYAY, R.P. TRIPATHI, A. TRIPATHI, A.D. SHUKLA & N. BHANDARI (2001). Nano-sized iron phases at the K/T and P/T boundaries revealed by Mössbauer spectroscopy. *Lunar and Planetary Science Conference XXXII,* LPI contribution 1270.

VILLASANTE-MARCOS, V., F. MARTÍNEZ-RUIZ, M.L. OSETE & J. URRUTIA-FUCUGAUCHI (2007). Magnetic characterization of Cretaceous-Tertiary boundary sediments. *Meteoritics and Planetary Science* 42, 1505-1527.

WDOWIAK, T.J., L.P. ARMENDAREZ, D.G. AGRESTI, M.L. WADE, S.Y. WDOWIAK, PH. CLAEYS & G. IZETT (2001). Presence of an iron-rich nanophase material in the upper layer of the Cretaceous-Tertiary boundary clay. *Meteoritics & Planetary Science* 36, 123-133.

WORM, H.U. & S.K. BANERJEE (1987). Rock magnetic signature of the Cretaceous-Tertiary boundary. *Geophysical Research Letters* 14, 1083-1086.